3.3 Strongly Correlated Quantum Systems

Unified understanding of the non-monotonic T_c variance of the 1111 iron pnictide superconductors

KAZUHIKO KUROKI
Department of Physics, Osaka University
1-1 Machikaneyama, Toyonaka, Osaka, 560-0043, Japan

Recently, non-monotonic variance of the T_c against chemical substitution is observed in some 1111 iron-based superconductors. We have theoretically investigated the origin of such variances taking into account the change in the band structure with chemical substition.

ARSENIC PHOPHORUS ISOVALENT DOPING SYSTEMS

In isovalent doping system LaFe(As,P)(O,F), recent experiments show that T_c is first suppressed as the phosphorus content is increased, but then it is re-enhanced and takes a local maximum at some P/As ratio.[1–3] As the phosphorus content is increased and the Pn-Fe-Pn bond angle increases, the d_{xy} hole Fermi surface is expected to be lost, and the top of the d_{xy} band moves away from the Fermi level. Therefore, the d_{xy} band contribution to the spin fluctuation decreases monotonically as the phosphorus content increases, especially after the d_{xy} Fermi surface disappears. The spin-fluctuation-mediated pairing is strongly degraded when the d_{xy} hole Fermi surfaces is absent, suggesting that the d_{xy} band plays an important role in the occurrence of high T_c superconductivity. Nonetheless, our recent calculation shows that T_c of the spin-fluctuation-mediated pairing shows a non-monotonic behavior even after the d_{xy} hole Fermi surface is lost; it exhibits a local maximum around a certain phosphorus content (i.e., certain Pn-Fe-Pn bond angle) greater than that at which the d_{xy} Fermi surface disappears, as shown in Fig.1(a)[4]. The origin of this non-monotonic variance is traced back to the fact that the disappearance of the d_{xy} hole Fermi surface leads to a better nesting within the $d_{xz/yz}$ portion of the Fermi surface, thereby enhancing the low lying spin excitations. It is also found in our calculation that the Pn-Fe-Pn bond angle at which the T_c is locally maximized decreases when the electron doping rate is increased. These results are consistent with recent experimental observations [1–3]. This indicates that the $d_{xz/yz}$ orbitals by themselves can play the main role in the occurrence of spin-fluctuation-mediated superconductivity, although the T_c in those cases is not very high.

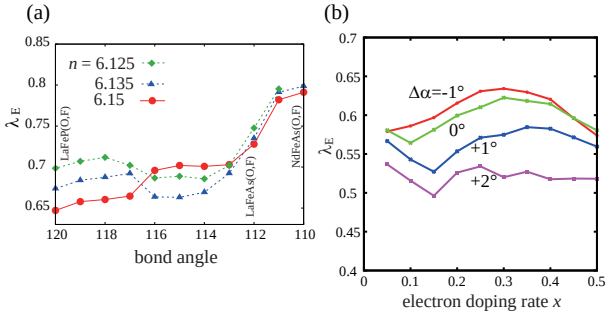

FIG. 1. (a) Eigenvalue of the linearized Eliashberg equation λ_E plotted against the hypothetically varied Pn-Fe-Pn bond angle for the model of LnFe(As,P)(O,F). n is the electron density and $n-6$ corresponds to the electron doping rate (taken from [4]). (b) λ_E plotted against the electron doping rate for the model of LnFe(As,P)(O,H). $\Delta\alpha$ is the Pn-Fe-Pn bond angle deviation with respect to that of LaFeAsO (taken from [8]). In both (a) and (b), λ_E can be considered as a qualitative measure for T_c , and smaller bond angle corresponds to smaller P/As content ratio or replacing the rare earth as La→ Nd or Sm. for s±-wave pairing

HYDROGEN DOPED SYSTEMS

In the hydrogen doped system $LaFeAsO_{1-x}H_x$, electron doping rate can exceed 50 percent, and the T_c phase diagram against the doping rate x exhibits a double dome structure, where the second dome with higher doping concentration has the higher T_c[5]. In a rigid band picture, such a large amount of electron doping would wipe out the hole Fermi surfaces, so that the Fermi surface nesting would no longer be good in the higher T_c second dome. However, first principles band calculation that takes into account the band structure variation with chemical substitution reveals that the band structure rapidly changes with doping, and the rigid band picture is not valid[6–8]. In momentum space, the $d_{xz/yz}$ hole Fermi surfaces around (0,0) shrink monotonically and are eventually lost with sufficient electron doping, and in turn an electron Fermi surface appears. On the other hand, an interesting point is that the d_{xy} hole Fermi surface around (π,π) is barely changed with the doping rate x, which is clearly a non-rigid band feature. Surprisingly, this is due to a rapid decrease of t_1

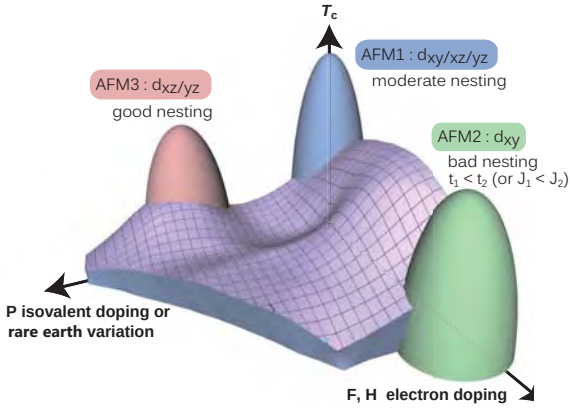

FIG. 2. A theoretical interpretation of the superconducting phase diagram of the 1111 family (taken from [4]).

within the d_{xy} orbital upon increasing x, which pushes up the d_{xy} band top at (π, π), so that it follows the increase of the Fermi level.

As seen in the above, the d_{xy} hole Fermi surface remains even at large electron doping rate, while the $d_{xz/yz}$ hole Fermi surfaces are lost, so that the importance of the d_{xy} orbital increases with doping. Interestingly, our fluctuation exchange study of these non-rigid band models show that the spin fluctuation and the s $\pm$ pairing are both enhanced in this largely doped regime, exhibiting a double dome feature of the superconducting T_c as a function of doping. Moreover, the two domes are merged into a single dome when the Pn-Fe-Pn bond angle is reduced (a change that takes place when the rare earth is varied as La→Ce→Sm→Gd), as shown in Fig.1(b), in agreement with the experiment. Although the d_{xy} hole Fermi surface remains unchanged in the highly doped regime, the Fermi surface nesting (in its original sense of the term) is monotonically degraded because the volume of the electron Fermi surfaces increases, so the origin of the second dome in $LaFeAsO_{1-x}H_x$ cannot be attributed to a good Fermi surface nesting. Here one should recall that s $\pm$ pairing is a next nearest neighbor pairing, which is favored by the relation between nearest and next nearest neighbor antiferromagnetic interactions $J_2 > J_1$, corresponding to $t_2 > t_1$. In fact, as mentioned above, t_2 dominating over t_1 is what is happening in the second T_c dome regime. Hence, intuitively, $t_2 > t_1$ can be considered as the origin of the T_c enhancement in the largely doped regime. To be precise, however, the fluctuation exchange approximation is a weak coupling method based on the itinerant spin model, so using the $J_1 - J_2$ term of the localized spin model is not conceptually correct. In reality, the entire d_{xy} portion of the band structure is strongly modified in a manner that it favors the second nearest neighbor pairing.

An important point here is that the t_1 reduction is largely due to the increase of the positive charge within the blocking layer by O(2-)→H(1-) substitution, which in turn reduces the As $4p$ electronic level and leads to the suppression of the indirect component of t_1[8]. Interestingly, we have recently found that a similar situation can occur when pressure is applied to some of the iron-based superconductors. The study on this problem is now in progress.

CONCLUSION

The hydrogen doped case shows that a good Fermi surface nesting is not necessary for the spin fluctuation mediated pairing even in the itinerant spin picture. On the other hand, in the isovalent doping system, the nesting of the $d_{xz/yz}$ Fermi surface can enhance the pairing. In total, the nesting and s $\pm$ superconductivity can in some cases be correlated with the Fermi surface nesting, while in other cases not. This also explains why the strength of the low energy spin fluctuation probed by NMR is in some cases correlated with T_c, while in other cases not, because the low energy spin fluctuation is largely governed by the Fermi surface nesting. We have summarized these theoretical interpretations in Fig.2.

[1] S. Miyasaka, A.Takemori, T. Kobayashi, S. Suzuki, S. Saijo, S. Tajima, J. Phys. Soc. Jpn. 82, 124706 (2013).
[2] K. T. Lai, A. Takemori, S. Miyasaka, F. Engetsu, H. Mukuda, S. Tajima, Phys. Rev. B 90, 064504 (2014).
[3] H. Mukuda, F. Engetsu, K. Yamamoto, K. T. Lai, M. Yashima, Y. Kitaoka, A. Takemori, S. Miyasaka, S. Tajima, Phys. Rev. B 89, 064511, (2014).
[4] H. Usui, K. Suzuki, and K. Kuroki, arXiv:1501.06303.
[5] S. Iimura, S. Matsuishi, H. Sato, T. Hanna, Y. Muraba, S.W. Kim, J. E. Kim, M. Takata and H. Hosono, Nat. Commun. 3, 943 (2012).
[6] S. Iimura, S. Matsuishi, M. Miyakawa, T. Taniguchi, K. Suzuki, H. Usui,K. Kuroki, R. Kajimoto, M. Nakamura, Y. Inamura, K. Ikeuchi, S. Ji, and H. Hosono, Phys. Rev. B, 060501(R) (2013).
[7] K. Suzuki, H. Usui, K. Kuroki, S. Iimura, Y. Sato, S.Matsuishi, and H. Hosono, J. Phys. Soc. Jpn. 82, 083702 (2013).
[8] K. Suzuki, H.Usui, S. Iimura, Y. Sato, S. Matsuishi, H. Hosono, and K. Kuroki Phys. Rev. Lett. 113, 027002 (2014)

Numerical studies on novel realistic quantum phases induced by cooperative spin-orbit couplings and electron correlations

Masatoshi IMADA

Department of Applied Physics, University of Tokyo,
7-3-1, Hongo, Bunkyo-ku, Tokyo 113-8786, Japan

Topological aspects in electronic structure of materials have been an intensively studied subject in recent research in condensed matter physics. In particular, interplay of spin-orbit interaction and electron correlations has revealed unprecedented and rich properties in a number of iridium oxides which is known as touchstone compounds of the interplay.

We have extended studies on an iridium oxide with the honeycomb structure, Na_2IrO_3 based on first principles. Na_2IrO_3 was proposed to show a novel Kitaev spin liquid [1], while experimental observation has established the zig-zag type magnetic order [2]. Our first principles study has reproduced the observed zig-zag type order [3]. In this project, we have further shown that the neutron scattering measurements, and thermodynamic properties are quantitatively consistent with the results calculated from the first principles study. The way to reach the Kitaev spin liquid has also been examined.

In this activity report, we summarize studies on another series of iridium oxides, with the pyrochlore lattice structure $A_2Ir_2O_7$ with A being rare earth elements, where predictions on novel topological properties at the domain wall of their magnetically ordered phase have been made [4].

$A_2Ir_2O_7$ with A being rare earth elements was first predicted to have an all-in-all-out (AIAO) type antiferromagnetic order in case of A =Y [5] and experimentally confirmed for A =Nd and Y [6]. This AIAO order is expected to host Weyl fermions in the bulk. Although the Weyl fermion is fragile when the magnetic order grows, magnetic domain walls offer topologically novel interfaces [4].

Namely, we have theoretically predicted that a class of magnetic domain walls induces unexpected interface metals accompanied by a net uniform magnetization around the domain wall, in the background of seemingly trivial bulk antiferromagnetic insulator, where uniform magnetization is cancelled each other in the bulk. The metallicity of the domain wall is substantiated by the formation of Fermi arcs at the domain walls, which have originally been formed by the Weyl electrons. The Fermi arc evolves into the Fermi surface when the Weyl fermions are eliminated. We have revealed that the magnetic domain walls of the AIAO phase are characterized by a zero-dimensional class A Chern number [4].

The electron correlation not only plays a crucial role in the formation of the AIAO order but also subsequent phase transitions emerging in the two-dimensional electrons at the domain wall. We have predicted that the metallic electrons have a helical nature at the fermi surface with some similarity to the Rashba metals. We have shown by using an effective hamiltonian, the helical nature induces an anomalous Hall conductivity, circular dichroism, and optical Hall conductivity under external magnetic fields. By increasing the electron correlation, the metallic domain wall states undergo the phase transitions from a degenerate helical metal to a spontaneously symmetry-broken helical metal, where the product of the inversion and time reversal symmetry is broken. With further increasing the interaction, it eventu-

ally becomes a topologically trivial antferromagnetic insulator even at the domain wall.

This work has been done in collaboration with Youhei Yamaji.

References

[1] G. Jackeli and G. Khaliullin, Phys. Rev. Lett. **102** (2009) 017205; J. Chaloupka, G. Jackeli, and G. Khaliullin, Phys. Rev. Lett. **105** (2010) 027204.

[2] S. K. Choi *et al.*, Phys. Rev. Lett. **108** (2012) 127204; F.Ye *et al.*, Phys. Rev. B **85** (2012) 180403.

[3] Y. Yamaji, Y. Nomura, M. Kurita, R. Arita and M. Imada, Phys. Rev. Lett. **113** (2014) 107201.

[4] Y. Yamaji and M. Imada, Phys. Rev. X **4** (2014) 021035.

[5] X. Wan, A. M. Turner, A. Vishwanath, and S. Y. Savrasov, Phys. Rev. B **83** (2011) 205101.

[6] K. Tomiyasu, *et al.*, J. Phys. Soc. Jpn. **81** (2012) 034709; H. Sagayama *et al.*, Phys. Rev. B **87** (2013) 100403.

Intersite electron correlations in two-dimensional Hubbard Penrose Lattice

AKIHISA KOGA
Department of Physics, Tokyo Institute of Technology
Meguro, Tokyo 152-8551, Japan

Quasiperiodic systems have attracted considerable interest since the discovery of quasicrystals. One of the specific features is the existence of a long-range order without translational symmetry. Recently, interesting low-temperature properties have been observed in the quasicrystal $Au_{51}Al_{34}Yb_{15}$ and its approximant $Au_{51}Al_{35}Yb_{14}$ [1]. In the former compound, the specific heat and susceptibility exhibit power-law behavior with a nontrivial exponent at low temperatures. In contrast, the approximant with the periodic structure shows conventional heavy fermion behavior. These findings suggest that electron correlations and quasiperiodic structure play a crucial role in stabilizing quantum critical behavior at low temperatures. Therefore, it is desirable to clarify how electron correlations affect low-temperature properties in quasiperiodic system.

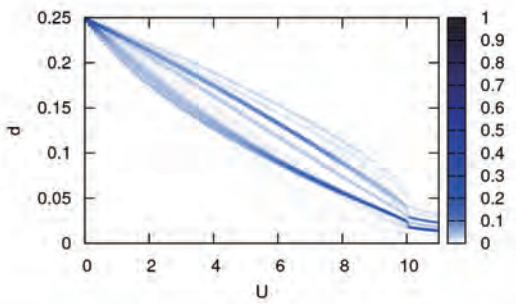

Figure 1: Density plot of double occupancy as a function of interaction strength U in the half-filled Penrose-Hubbard model with 4481 sites when $T = 0.05$.

Motivated by this, we have investigated the half-filled Hubbard model on the two-dimensional Penrose lattice, combining the Real-space DMFT[2] with the CTQMC method. Computing the double occupancy and renormalization factor at each site, we have discussed the Mott transition at finite temperatures. Furthermore, we have found that the quasiparticle weight strongly depends on the site and its geometry[3]. However, intersite correlations cannot be taken into account with RDMFT. In the present work, we developed Dual Fermion approarch[4] where inter-site correlations in inhomogeneous system are taken into account. We will investigate how magnetic fluctuations develop in quasiperiodic system.

References

[1] K. Deguchi, S. Matsukawa, N. K. Sato, T. Hattori, K. Ishida, H. Takakura, and T. Ishimasa, Nat. Mater. **11**, 1013 (2012).

[2] A. Georges, G. Kotliar, W. Krauth, and M. J. Rozenberg, Rev. Mod. Phys. **68**, 13 (1996).

[3] N. Takemori, A. Koga, J. Phys. Soc. Jpn. **84**, 023701 1-5 (2015).

[4] A. N. Rubtsov et al., Phys. Rev. B 77, 033101 (2008).

Stability of the superfluid state with internal degree of freedom

AKIHISA KOGA
Department of Physics, Tokyo Institute of Technology
Meguro, Tokyo 152-8551, Japan

Superfluid state in ultracold atomic systems has attracted current interest. Recently, fermionic systems with internal degrees of freedom have experimentally been realized [1, 2, 3], which stimulates further theoretical investigation on the superfluid state in multicomponent fermionic systems [4, 5]. Since the fermionic system with even number of components should be equivalent to the strongly correlated electron systems with degenerate orbitals, it is highly desired to discuss how the superfluid state is realized in these systems.

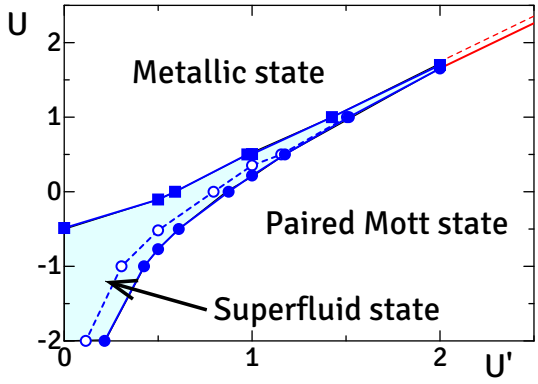

Figure 1: Phase diagram of the four-component Fermionic system equivalent to the degenerate orbital system with intraorbital (interorbtial) Coulomb interaction U (U') at $T = 0.01$.

Motivated by this, we have studied low temperature properties of the degenerate Hubbard model with the intra- and interorbital Coulomb repulsions, which is equivalent to the four component fermionic system. By combining dynamical mean-field theory with a continuous-time quantum Monte Carlo method, we have obtained the finite temperature phase diagram, as shown in Fig. 1. We have found that the s-wave superfluid state realized by the attractive interaction U is adiabatically connected to that in the repulsive interacting region [6]. It is expected that this superfluid state should capture the essence of the superconducting state in the fullerene-based solid A_3C_{60}. It is an interesting problem to clarify this point, which is now under consideration.

References

[1] T. B. Ottenstein et al., Phys. Rev. Lett. **101** 203202 (2008).

[2] T. Fukuhara et al., Phys. Rev. Lett. **98**, 030401 (2007).

[3] B. J. DeSalvo et al., Phys. Rev. Lett. **105**, 030402 (2010).

[4] K. Inaba and S. Suga, Phys. Rev. Lett. **108**, 255301 (2012); K. Inaba and S. Suga, Mod. Phys. Lett B **27**, 1330008 (2013).

[5] Y. Okanami, N. Takemori and A. Koga, Phys. Rev. A **89**, 053622 (2014).

[6] A. Koga and P. Werner, Phys. Rev. B **91**, 085108 (2015).

Unified description of the electronic properties of Sr_2RuO_4 in a paramagnetic phase

Naoya ARAKAWA
Center for Emergent Matter Science, RIKEN
Wako, Saitama 351-0198

Correlated multiorbital systems show various electronic properties due to the combination of electron correlation and complex degrees of freedom such as charge, spin, and orbital. Examples are anisotropic superconductivity, giant magnetoresistance effect, and non-Fermi-liquid-like behaviors. Among several correlated multiorbital systems, ruthenates have rich electronic states, depending on the crystal structure or the chemical composition or both. For example, Sr_2RuO_4 becomes a spin-triplet superconductivity at very low temperatures, Ca_2RuO_4 becomes a Mott insulator, and $Sr_2Ru_{0.075}Ti_{0.025}O_4$ becomes a nearly-antiferomagnetic metal. Since those electronic states are realized in other correlated multiorbital systems and the basic electronic structure of ruthenates is simpler, research on ruthenates is suitable to understand the roles of electron correlation and complex degrees of freedom in a correlated multiorbital system.

Despite extensive research, the electronic properties of Sr_2RuO_4 even in a paramagnetic phase have not been correctly understood. It is experimentally established that Sr_2RuO_4 is categorized into a quasi-two-dimensional t_{2g}-orbital system with moderately strong electron correlation. In addition, the temperature dependence of the physical quantities such as the spin susceptibility and the inplane resistivity are the same as those in Landau's Fermi liquid theory. However, there have been several remaining problems such as the origin of the larger mass enhancement of the d_{xy} orbital than that of the $d_{xz/yz}$ orbital.

In this project, I studied several electronic properties of Sr_2RuO_4 using the fluctuation-exchange approximation with the current vertex corrections arising from the self-energy and Maki-Thompson four-point vertex function due to electron correlation for a t_{2g}-orbital Hubbard model on a square lattice and achieved the satisfactory unified description of the low-temperature electronic properties [1, 2], which are the larger mass enhancement of the d_{xy} orbital, the strongest enhancement of the spin fluctuation at $\boldsymbol{q} \approx (\frac{2}{3}\pi, \frac{2}{3}\pi)$, the crossover of the inplane resistivity from the T dependence to the T^2 dependence at low temperature, and the nonmonotonic temperature dependence of the Hall coefficient including an appearance of a peak at low temperature; the agreement in the orbital dependence of the mass enhancement is better than that in case of the dynamical-mean-field theory. This study [1, 2] leads to taking an important step towards understanding the characteristic roles of electron correlation and complex degrees of freedom in ruthenates and the ubiquitous properties of correlated multiorbital systems.

References

[1] N. Arakawa: Phys. Rev. B **90** (2014) 245103.

[2] N. Arakawa: arXiv:1503.06937; accepted for publication in Modern Physics Letters B as an invited brief review article.

Microscopic theory on charge transports of a correlated multiorbital system

Naoya ARAKAWA
Center for Emergent Matter Science, RIKEN
Wako, Saitama 351-0198

Many-body effects are important to discuss the electronic properties of correlated electron systems. For several correlated electron systems, Landau's Fermi liquid (FL) theory describes many-body effects in terms of quasiparticles. In this theory, the temperature dependence of the physical quantities are the same as those in noninteracting case and many-body effects are the changes of its coefficient due to the mass enhancement or the FL correction or both. However, for correlated electron systems near a magnetic quantum-critical point (QCP), many-body effects cause non-FL-like behaviors, the deviations from the temperature dependence expected in Landau's FL theory; for example, in $Sr_2Ru_{0.075}Ti_{0.025}O_4$, which is located near an antiferromagnetic (AF) QCP, the spin susceptibility shows the Curie-Weiss-like behavior and the resistivity shows the T-linear dependence. Thus, the emergence of such non-FL-like behaviors indicates the importance of discussing many-body effects beyond Landau's FL theory.

However, many-body effects in correlated multiorbital systems have been little understood compared with understanding many-body effects in correlated single-orbital systems. This is because of difficulty taking the enough numbers of the mesh of the Brillouin zone and the Matsubara frequency in the presence of orbital degrees of freedom for the numerical calculations including many-body effects; the enough numbers are necessary to obtain reasonable results of the electronic properties at low temperatures without the problematic numerical errors due to the finite size effects. This large numerical cost becomes severer for storing two-particle quantities such as the susceptibility in a spin sector than for storing single-particle quantities such as the self-energy since the two-particle quantity has four orbital indices, which is twice as large as the orbital indices of the single-particle quantity.

With the above background, I formulated the resistivity and the Hall coefficient in the weak-field limit for a multiorbital Hubbard model using the linear-response theory and the extended Éliashberg theory and adopted this method to the inplane charge transports of paramagnetic (PM) quasi-two-dimensional ruthenates away from and near the AF QCP in combination with the fluctuation-exchange (FLEX) approximation with the current vertex correction (CVC) arising from the self-energy and the Maki-Thompson (MT) four-point vertex function for the t_{2g}-orbital Hubbard model on a square lattice [1, 2]. To my knowledge, this [1] is the first research to study the transport properties of a correlated multiorbital system including the CVCs arising from the self-energy and four-point vertex function due to electron correlation. From a technical point of view, I resolved the numerical difficulty explained above by using the symmetry of the system and utilizing the arrays efficiently, resulting in the reductions of the memory of the arrays and the time of the numerical calculations.

There were several remaining issues in my previous studies [1, 2], although I succeeded in reproducing several experimental results of Sr_2RuO_4 and $Sr_2Ru_{0.075}Ti_{0.025}O_4$ satisfactorily and obtaining several characteristic aspects of a correlated multiorbital system. Among those remaining issues, it is highly desirable to clarify the main effects of the CVC arising from the Aslamasov-Larkin (AL) four-point vertex function on the inplane charge transports. In the previous studies [1, 2], I neglected the AL CVC since I assumed that the CVCs arising from the self-energy and the MT four-point vertex function are sufficient for qualitative discussions. This is because it is known in a single-orbital Hubbard model on a square lattice [3] that the AL CVC does not qualitatively change the transport properties near an AF QCP since the MT CVC is more important. However, it is unclear whether the AL CVC keeps the results obtained in the previous studies qualitatively unchanged since there has been no previous research to study its effects in a correlated multiorbital system. Thus, it is necessary to check the validity of the assumption used in the previous studies. Furthermore, the analysis of the effects of the AL CVC is important for a deeper understanding of the roles of the CVCs in a correlated multiorbital system since not only the MT but also the AL CVC is vital to hold conservation laws.

Due to the above importance to clarify the main effects of the AL CVC, I studied these effects by considering the main terms of the AL CVC in this project [4]. As a result, I showed that the results of the previous studies remain qualitatively unchanged even including the main terms of the AL CVC and obtained several important results. The most important result is finding the existence of two distinct regions of the temperature dependence of the transport properties near the AF QCP: in low temperature region, the CVCs arising from the self-energy and the MT four-point vertex function are sufficient even in a quantitative level; in high temperature region, the CVC arising from the self-energy is sufficient since the effects of the MT and the AL CVC are nearly cancelled out. Although the existence of the former region was pointed out about 16 years ago by H. Kontani *et al.* [3] on the basis of the analytic discussion, it is important to show the existence of the two distinct region in the numerical calculations for a deeper understanding of the effects of the CVCs. In addition, this finding gives a useful guide to choose the simple theory that is sufficient to study the transport properties.

Since the developments of the computational resources are one of the vital factors to achieve the above important result, it is very important to continue providing the computational resources of the Supercomputer Center at the Institute for Solid State Physics in order to develop our understanding of many-body effects in a correlated electron system.

References

[1] N. Arakawa: Phys. Rev. B **90** (2014) 245103.

[2] N. Arakawa: arXiv:1503.06937; accepted for publication in Modern Physics Letters B as an invited brief review article.

[3] H. Kontani, K. Kanki, and K. Ueda: Phys. Rev. B **59** (1999) 14723.

[4] N. Arakawa: in preparation.

Quantum Phase Transition in the Hubbard Model on the CaV_4O_9 lattice

Yuki Yanagi
Department of Physics, Faculty of Science and Technology, Tokyo University of Science
Noda, Chiba 278-8510

CaV_4O_9 is a well-known typical example of spin-gapped systems[1]. The minimal model for CaV_4O_9, the Heisenberg model on the 1/5-depleted square lattice shows two distinct spin gapped phases depending on values of J_1 and J_2, where J_1 and J_2 are the intra-plaquette and intra-dimer couplings, respectively[2].

Inspired by the results of the Heisenberg model, we have investigated the nonmagnetic Mott transition in the itinerant model on the same lattice, the 1/5-depleted square lattice Hubbard model at half-filling[3]. In this project, we have revealed the nature of the Mott transition for $t_1 < t_2$ by using the 8-site cellular dynamical mean field theory (CDMFT), where t_1 and t_2 are the intra-plaquette and intra-dimer hoppings, respectively (see Fig. 1). In the CDMFT, a lattice problem is mapped onto a cluster one with open boundary conditions embedded in a electronic bath which is self-consistently determined. We have employed the auxiliary field continuous-time quantum Monte Carlo method (CT-AUX) as the cluster solver[4]. This numerically exact method is based on a decoupling of the on-site Coulomb interaction term by auxiliary Ising spins and a weak coupling expansion of the partition function. Although the CT-AUX is suitable for the cluster solver with large cluster sizes, numerical calculations at low temperatures and for large Coulomb interactions U are rather time-consuming. Therefore, to reduce the computation time, we have performed the parallel calculation in system-B. We have calculated the double occupancy d, electron self-energy and one-particle Green's function. We have found that the Mott transition occurs without any discontinuous jumps in U-d curves and clarified that the transition is nothing but a Lifshitz transition driven by the dimerization due to the non-local correlation effects.

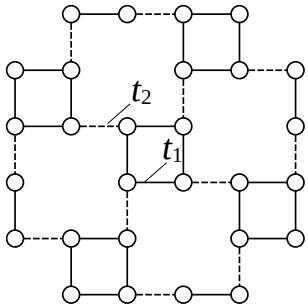

Figure 1: Schematic of the 1/5-depleted square lattice.

This work was done in collaboration with Prof. K. Ueda.

References

[1] S. Taniguchi *et al.*, J. Phys. Soc. Jpn. **64**, 2758 (1995).

[2] K. Ueda *et al.*, Phys. Rev. Lett. **76**, 1932 (1996)

[3] Y. Yanagi and K. Ueda, Phys. Rev. B **90**, 085113.

[4] E. Gull *et al.*, Rev. Mod. Phys. **83**, 349.

Multipolar excitations in pyrochlore systems

MASAFUMI UDAGAWA
Department of Physics, Gakushuin University
1-5-1 Mejiro, Toshima-ku, Tokyo, 171-8588

Recently, multipole ordering has been drawing considerable interest as a driving force of novel multiferroic response and anomalous transport phenomena. We have pursued the realization of multipole ordering in systems with frustrated pyrochlore structure and their variants, and found several ordering patterns, as well as the existence of nontrivial multipolar excitations.

Among many multipole orderings, here we focus on the toroidal excitation realized in the nonequilibrium process in pyrochlore spin ice system. Spin ice is a prototypical frustrated magnet, with a number of remarkable features, such as groundstate degeneracy, fractional monopole excitations, and quasi-long range correlation, which now serve as fundamental concepts to understand frustrated magnetism in general. Among these properties, dynamical character of spin ice has drawn a considerable attention. Indeed, in dipolar spin ice, drastic divergence of relaxation time has been observed at low temperatures, and it has been revealed theoretically that monopole excitations play a key role in the slow dynamics.

In a variant of spin ice model, J_1-J_2-J_3 spin ice model, the monopole exceptions interact with each other via short-range forces. We analyzed the classical dynamics of this model with a waiting-time Monte Carlo method, and clarified the time evolution of monopole density and magnetization for all the range of $J_2 = J_3 \equiv J$. In particular, we found several quasi-stable macroscopic states survive as a steady state with macroscopically long relaxation time, even though they have higher energy compared with ground state. Among them, we found a collective excitation which we term "monopole jellyfish" (1). This monopole jellyfish excitation possesses a troidal spin structure, and can be regarded as a sort of multipole excitation. This excitation may give a crucial clue to the spontaneous Hall effect [1] observed in $Pr_2Ir_2O_7$, which is known as a metallic spin ice [2].

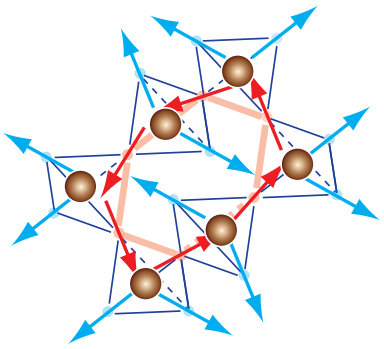

図 1: Schematic figure of monopole jellyfish.

参考文献

[1] Y. Machida et al., Nature **463**, 210 (2010).

[2] M. Udagawa, L. D. C. Jaubert, C. Castelnovo and R. Moessner, in preparation

Research on Kondo effect in electron-phonon systems by numerical renormalization group method

Takashi HOTTA
Department of Physics, Tokyo Metropolitan University
1-1 Minami-Osawa, Hachioji, Tokyo 192-0397

In this research, we discuss the Kondo effect in a spinless two-orbital conduction electron system coupled with anharmonic Jahn-Teller vibration by employing a numerical renormalization group technique [1]. When a temperature T is decreased, we encounter a plateau of $\log 3$ entropy due to quasi-triple degeneracy of local low-energy states, composed of vibronic ground states and the first excited state with an excitation energy of ΔE. Around at $T \approx \Delta E$, we observe an entropy change from $\log 3$ to $\log 2$. This $\log 2$ entropy originates from the rotational degree of freedom of the vibronic state and it is eventually released due to the screening by orbital moments of conduction electrons, leading to the Kondo effect of a Jahn-Teller ion.

The Hamiltonian for electrons coupled with anharmonic Jahn-Teller vibration is given by

$$\begin{aligned} H_0 = {} & g(\tau_x Q_2 + \tau_z Q_3) + (P_2^2 + P_3^2)/(2M) \\ & + A(Q_2^2 + Q_3^2) + B(Q_3^3 - 3Q_2^2 Q_3) \\ & + C(Q_2^2 + Q_3^2)^2, \end{aligned}$$

where g is the electron-vibration coupling constant, $\tau_x = d_a^\dagger d_b + d_b^\dagger d_a$, $\tau_z = d_a^\dagger d_z - d_b^\dagger d_b$, d_τ is the annihilation operator of spinless fermion with orbital τ, a and b correspond to $x^2 - y^2$ and $3z^2 - r^2$ orbitals, respectively, M is the reduced mass of Jahn-Teller oscillator, Q_2 and Q_3 denote normal coordinates of $(x^2 - y^2)$- and $(3z^2 - r^2)$-type Jahn-Teller oscillation, respectively, P_2 and P_3 indicate corresponding canonical momenta, A indicates the quadratic term of the potential, and B and C are, respectively, the coefficients for third- and fourth-order anharmonic terms. Note that we consider only the anharmonicity which maintains the cubic symmetry. Here we consider the case of $A > 0$ and $C > 0$, while B takes both positive and negative values.

After some algebraic calculations, we obtain

$$\begin{aligned} H_0 = {} & \sqrt{\alpha}\omega[(a_2 + a_2^\dagger)\tau_x + (a_3 + a_3^\dagger)\tau_z] \\ & + \omega(a_2^\dagger a_2 + a_3^\dagger a_3 + 1) + \beta\omega[(a_3 + a_3^\dagger)^3 \\ & - 3(a_2 + a_2^\dagger)^2(a_3 + a_3^\dagger)]/3 \\ & + \gamma\omega[(a_2 + a_2^\dagger)^2 + (a_3 + a_3^\dagger)^2]^2/8, \end{aligned}$$

where ω is the vibration energy, given by $\omega = \sqrt{2A/M}$, a_2 and a_3 are annihilation operators of phonons for Jahn-Teller oscillations, α is the non-dimensional electron-phonon coupling constant, given by $\alpha = g^2/(2M\omega^3)$, β and γ are non-dimensional anharmonicity parameters, defined by $\beta = 3B/[(2M)^{3/2}\omega^{5/2}]$ and $\gamma = 2C/(M^2\omega^3)$, respectively.

Note that it is important to consider the parity for phonon vibration, when we determine the properties of phonon states more precisely. However, such a discussion is meaningful only in the high-temperature region, and so we do not mention it anymore in this report, since we are interested only in the low-temperature properties of Kondo phenomena. Here we remark the appearance of the peculiar chaotic properties of the anharmonic Jahn-Teller vibration in the high-temperature region [2].

Now we consider the conduction electron hybridized with localized electrons. Then, the

model is expressed as

$$H = \sum_{\boldsymbol{k}\tau} \varepsilon_{\boldsymbol{k}} c^{\dagger}_{\boldsymbol{k}\tau} c_{\boldsymbol{k}\tau} + \sum_{\boldsymbol{k}\tau} (V c^{\dagger}_{\boldsymbol{k}\tau} d_{\tau} + \text{h.c.}) + H_0,$$

where $\varepsilon_{\boldsymbol{k}}$ is the dispersion of conduction electron, $c_{\boldsymbol{k}\tau}$ is an annihilation operator of conduction electron with momentum $\boldsymbol{k}$ and orbital τ, and V is the hybridization between conduction and localized electrons. The energy unit is a half of the conduction bandwidth, which is set as unity in the following.

To investigate the electronic and phononic properties of H at low temperatures, we usually discuss the corresponding susceptibilities, entropy, and specific heat. For the evaluation of these quantities, here, we employ the numerical renormalization group (NRG) method, in which the momentum space is logarithmically discretized to efficiently include the conduction electrons near the Fermi energy.

In Fig. 1, we show the typical NRG result of entropy and specific heat. In a high-temperature region, entropy is rapidly decreased with decreasing temperature T and it forms a plateau of $\log 3$ between $10^{-5} < T < 10^{-2}$. The origin of the $\log 3$ entropy is the quasi-degeneracy of local low-energy states, originating from the position degree of freedom of oscillation in the strong anharmonic potential with three minima. As easily understood from the above explanation, the quasi-triple degeneracy should be lifted at approximately $T = \Delta E$, where ΔE denotes the first excitation energy among local low-energy states. In fact, we observe a clear peak in the specific heat at $T \approx \Delta E$, since the entropy is changed from $\log 3$ to $\log 2$. The $\log 2$ entropy originates from the double degeneracy in the local vibronic states with double degeneracy, corresponding to clockwise and anticlockwise rotational directions. At a temperature where the rotational moment is screened by orbital moments of conduction electrons, the entropy of $\log 2$ is eventually released and a peak is formed in the specific heat. This peak naturally defines a characteristic temperature,

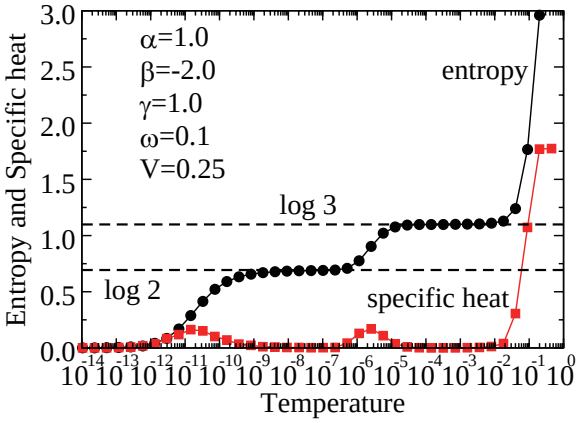

Figure 1: Entropy and specific heat for ω=0.1, α=1, β=−2, and γ=1.

which is called here the Kondo temperature $T_{\rm K}$. Due to the lack of the space, we do not show further results in this report, but it has been confirmed that $T_{\rm K}$ is well explained by the effective s-d model with anisotropic exchange interactions. As for details, readers should refer Ref. [1].

In summary, we have clarified the Kondo effect in the Jahn-Teller-Anderson model with cubic anharmonicity. We have found the $\log 3$ plateau in the entropy due to quasi-triple degeneracy in the low-energy states including vibronic ground states. With further decrease in temperature, we have observed the region of the $\log 2$ plateau due to the vibronic state with rotational degree of freedom. The rotational moment of the vibronic state has been found to be suppressed by the screening of orbital moments of conduction electrons, leading to the Kondo effect.

References

[1] T. Hotta, J. Phys. Soc. Jpn. **83**, 104706 (2014).

[2] T. Hotta and A. Shudo, J. Phys. Soc. Jpn. **83**, 083705 (2014).

Theoretical Analysis of Quantum Properties at Heterostructures and Superlattices of Strongly Correlated Systems

NORIO KAWAKAMI
Department of Physics, Kyoto University, Kyoto 606-8502, Japan

Starting with their experimental realization, multilayered heterostructures of strongly-correlated electron systems have attracted much attention among the primary topics in condensed matter physics. New aspects in this field have been revealed via recent work on $(LaVO_3)_n/(SrVO_3)_m$ perovskite superlattices, consisting of the periodically aligned $LaVO_3$ and $SrVO_3$ layers. The bulk $LaVO_3$ is a Mott insulating antiferromagnet, while $SrVO_3$ is a strongly correlated paramagnetic metal with one conducting d electron per V ion, which is changed into an insulator in the 2D thin film. The experiments on the $(LaVO_3)_n/(SrVO_3)_m$ superlattices have reported the following intriguing phenomena[1]. (i) The temperature dependence of the in-plane resistivity shows an anomalous peak structure around the characteristic temperature T^*. Particularly a Fermi liquid metallic behavior is observed sufficiently below T^*. In addition the magnitude of T^* is altered with inserting additional $SrVO_3$ layers between $LaVO_3$ layers. (ii) Other transport measurements detect occurrence of a MIT in $(LaVO_3)_n/(SrVO_3)_1$ superlattices with varying the number of $LaVO_3$ layers from one to three. Some theoretical attempts of understanding magnetic properties have already been made, but the nature of exotic transport properties are currently under discussion.

In this paper, we propose a microscopic mechanism resolving the issues of resistivity measurements on $(LaVO_3)_n/(SrVO_3)_m$ superlattices[2]. For this purpose, we study the Mott physics in a simple Hubbard superlattice model consisting of the Mott-insulating layers and metal layers. The computed resistivity is shown in Fig.1. It is seen that the 3D Fermi-liquid metallic state is realized for various choices of superlattice configuration with decreasing temperature. We find that electron correlation effects under the superlattice geometry are strongly influenced by the periodicity of the superlattice, and cause an even-odd oscillation in the quasi-particle weight depending on the number of metal layers. We further clarify that this dependence further induces the detectable difference in the electrical resistivity, which may be essential for understanding some key experiments. Our model provides a reasonable explanation for experiments on $(LaVO_3)_n/(SrVO_3)_m$, including a peak formation in the resistivity and also the occurrence of a metal-insulator transition.

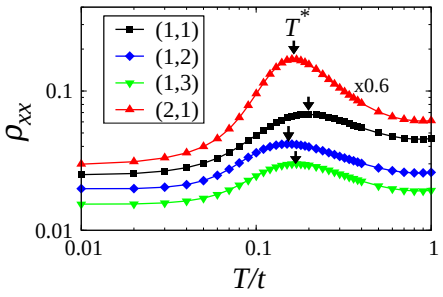

Figure 1: Temperature dependence of th in-plane resistivity ρ_{xx} for the (m, n) superlattices, where the unit cell consists of m Mott insulator layers and n metallic layers. The arrows show the peak position of the resistivity.

References

[1] A. David et al., Appl. Phys. Lett. **98**, 212106 (2011); U. Lueders et al., J Phys Chem Solids **75**, 1354 ((2014).

[2] S. Ueda and N. Kawakami, submitted.

Theoretical Studies of Correlation Effects for Quantum Phase Formation in Non-Homogeneous Systems

NORIO KAWAKAMI
Department of Physics, Kyoto University, Kyoto 606-8502, Japan

To reveal how interaction between particles influence physical properties has been a central issue in the past few decades. The influence caused by the spatial non-homogeneity has been also analyzed from 1958 when P. W. Anderson suggested the localization of electrons due to a random potential [1]. While it is expected that the competition or collaboration between these two effects might trigger novel physical phenomena, there are many open questions to this day.

Cold atoms in optical lattices have provided a great deal of control over system parameters. One can easily tune the strength of the interaction between particles by Feshbach resonance and also realize the systems with the spatial non-homogeneity by suitably combining different laser beams[2]. Therefore, the cold atomic systems provide an intriguing platform where one analyzes the competition(collaboration) between the interaction and the effects of the spatial non-uniformity.

One of the main issues in our research project is to study how the spatial non-uniformity affects the properties of the multi-component Fermi systems which are realized in cold atomic systems. We focus on the SU(N) attractive Fermi systems, where the interaction between the particles is independent of the components of particles. The SU(N) Fermi systems with the disordered potential in cold atoms are well-described by a SU(N) attractive Anderson-Hubbard model. It is known that the charge-density-wave (CDW) state and the s-wave superfluid (SF) state are degenerate in the SU(2) model without disorder at zero temperature and half-filling in a two-dimensional square lattice. Disorder lifts this degeneracy and hence stabilizes the SF state as a ground state. By contrast, for $N > 2$, in the absence of disorder the CDW state is stabilized as a ground state. Therefore, what kind of state is stabilized as the ground state in the SU($N > 2$) systems with disorder is an interesting open question.

To answer this question, we have first analyzed the SU(3) and SU(4) attractive Anderson-Hubbard model by using a real-space Bogoliubov-de Gennes(BdG) method. Within our method, the non-homogeneity of disordered systems is fully captured though we treat the effects of the attractive interaction as a mean-field. BdG equations are solved on a finite-size lattice and a disorder average of the physical quantities obtained by this method is taken. If the calculations are performed for smaller lattice sizes, we might overestimate the physical quantities corresponding to long-range orders, for example the superfluid order parameter, the charge structure factor, and so on. Also, a disorder average over only a small number of configurations might lead to erroneous conclusions owing to the sample dependence. For these reasons, the calculations are performed for lattice sizes up to 32×32, and the results are averaged over 12-40 different configurations in this study. To preform the large-scale numerical calculations, we have fully made use of the supercomputer resource at ISSP. Namely, we have performed large-scale parallel computing to diagonalize matrices with a large dimension.

The ground-state phase diagrams of the SU(3) and SU(4) cases have been obtained in this study [3]. The phase diagram for the SU(3) case is shown in Fig.1 and that for

SU(4) in Fig.2, respectively. From Fig.1, it is found that disorder triggers the CDW-SF transition at some disorder strength, and the SF-Anderson localized state(AL) transition occurs as the disorder strength further increases. Also, each critical disorder where the CDW-SF transition and the SF-AL transition occur increases as the strength of the attractive interaction increases. It is pointed out in this study that the CDW-SF transition and the SF-AL transition are of first order. The phase diagram for the SU(4) case indicates that the CDW state directly undergoes a transition to the AL. This result suggests that the SF state cannot be stabilized as a ground state in the SU(4) attractive Fermi systems with disorder at half-filling because the CDW state is rather stable and thus the energy gained by the SF order is not large enough to stabilize the superfluidity in between the CDW state and the AL.

However, the above conclusion has been drawn within the mean-field approximation. Hence it is important to evaluate the validity of this conclusion by using more accurate methods. For this purpose, we have performed additional calculations using quantum Monte Carlo simulations. The results obtained by these calculations will soon be reported elsewhere.

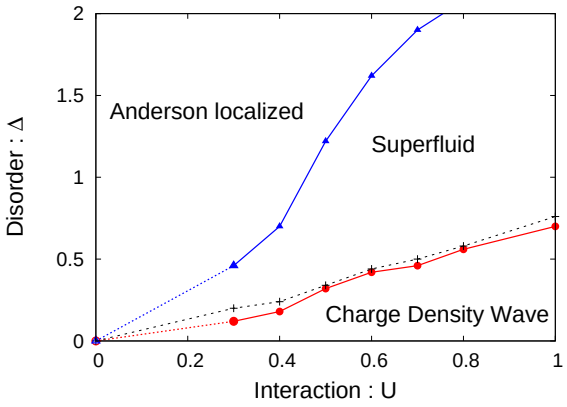

Figure 1: Ground-state phase diagram of the SU(3) attractive Anderson-Hubbard model. The red solid line with closed circles shows the CDW-SF transition points and the blue solid line with closed triangles the SF-AL transition points. The black dashed line denotes the points where the value of the free energy of the CDW state corresponds to that of the SF state.

References

[1] P. W. Anderson, Phys. Rev. **109**, 1492 (1958).

[2] J. E. Lye *et al.*, Phys. Rev. Lett. **95**, 070401 (2005).

[3] M. Sakaida *et al.*, Phys. Rev. A. **90**, 013632 (2014).

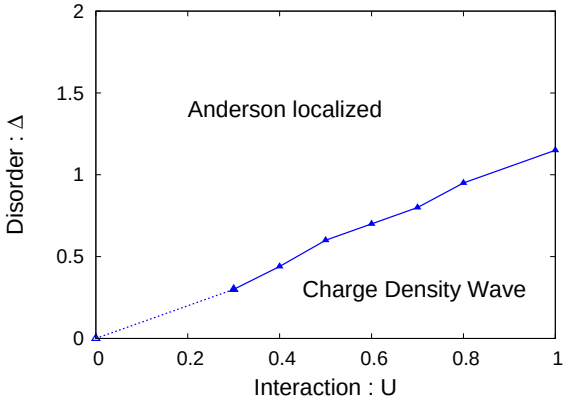

Figure 2: Ground-state phase diagram of the SU(4) attractive Anderson-Hubbard model. The CDW-AL transition points are denoted by the blue solid line with closed triangles.

Numerical Studies on Localization and Fractionalization of Many-Body Electrons with Strong Spin-Orbit Couplings

Youhei YAMAJI
Quantum-Phase Electronics Center, University of Tokyo
Hongo, Bunkyo-ku, Tokyo 113-8656

Theoretical prediction of emergent quantum phases in iridium oxides has stimulated both of experimental and further theoretical studies. Especially, a honeycomb lattice iridium oxide Na_2IrO_3 has attracted much attention as a candidate of the Kitaev's spin liquid. Recent experiments, however, show that the ground state of Na_2IrO_3 is a magnetically ordered insulator.

A remaining challenge is to realize the Kitaev's spin liquid by learning from Na_2IrO_3. First of all, we need to clarify what the effective hamiltonian of Na_2IrO_3 is. Then, we may understand how to design spin liquid materials.

By employing an *ab initio* scheme to derive low-energy effective hamiltonians based on the density functional theory, we construct an effective spin hamiltonian of Na_2IrO_3 given as a generalized Kitaev-Heisenberg model [1],

$$\hat{H} = \sum_{\Gamma=X,Y,Z} \sum_{\langle \ell,m \rangle \in \Gamma} \vec{\hat{S}}_\ell^T J_\Gamma \vec{\hat{S}}_m, \qquad (1)$$

where the bond-dependent exchange couplings are defined as

$$J_X = \begin{bmatrix} K' & I_2'' & I_2' \\ I_2'' & J'' & I_1' \\ I_2' & I_1' & J' \end{bmatrix},$$

$$J_Y = \begin{bmatrix} J'' & I_2'' & I_1' \\ I_2'' & K' & I_2' \\ I_1' & I_2' & J' \end{bmatrix},$$

$$J_Z = \begin{bmatrix} J & I_1 & I_2 \\ I_1 & J & I_2 \\ I_2 & I_2 & K \end{bmatrix}. \qquad (2)$$

Here we estimated these exchange couplings as $K = -30.7$ meV, $J = 4.4$ meV, $I_1 = -0.4$ meV, $I_2 = 1.1$ meV, $K' = -23.9$ meV, $J' = 2.0$ meV, $J'' = 3.2$ meV, $I_1' = 1.8$ meV, $I_2' = -8.4$ meV, and $I_2'' = -3.1$ meV.

Based on numerically simulated specific heat of the generalized Kitaev-Heisenberg model, we propose that half plateau structures of temperature-dependences of entropy are hallmarks of the Kitaev's spin liquids or quantum spin systems close to the Kitaev's spin liquids [1, 2].

We have examined the effective spin hamiltonian so far. However, Na_2IrO_3 is expected to be close to metal-insulator transitions. To clarify effects of itinerancy of electrons, we have recently developed a variational Monte Carlo method applicable to *ab initio* t_{2g} hamiltonian with strong spin-orbit couplings [3].

References

[1] Y. Yamaji, Y. Nomura, M. Kurita, R. Arita, and M. Imada: Phys. Rev. Lett. **113** (2014) 107201.

[2] Y. Yamaji: to appear in AIP Conference Proceedings.

[3] M. Kurita, Y. Yamaji, S. Morita, and M. Imada: arXiv:1411.5198.

Ab initio calculations for Mn analog of iron-based superconductors LaMnAsO and LaMnPO

Takahiro MISAWA

Department of Applied Physics, University of Tokyo,
7-3-1 Hongo, Bunkyo-ku, Tokyo 113-8656, Japan

In iron-based superconductors, although it is believed that electron correlations play key roles in stabilizing the high-temperature superconductivity, its role is not fully understand yet. Because iron-based superconductors are multi-orbital system (typically five d orbitals exist around the Fermi level), it is also suggested the orbital degrees of freedom play key role. To clarify microscopic mechanism of superconductivity in iron-based superconductors, it is necessary to evaluate strength of interactions in an *ab initio* way and it is also necessary to seriously examine the effects of electronic correlations. To challenge these issues, we employ *ab initio* downfolding scheme [1]. In this scheme, we first calculate the global band structures for target materials. Then, we eliminate high-energy degrees of freedom by using the constrained random-phase-approximation method and obtain the low-energy effective model. To solve the *ab initio* low-energy effective models, we use many-variable variational Monte Carlo method, which properly takes into account both spatial and dynamical quantum fluctuations. We applied this method to the iron-based superconductors and we showed that the calculated magnetic order was shown to correctly reproduce the experimental material dependences [2, 3].

In this project, by extending these normal state studies, we study how the superconductivity emerges in the low-energy effective model of an electron-doped iron-based superconductor LaFeAsO [4]. To solve the low-energy effective model, we mainly use the system B with hybrid parallelization (typically 8 OPENMP threads $\times$ 256 MPI processes). As a result, we show that superconductivity emerges in essential agreement with the experimental results. The pairing satisfies gapped $s_{\pm}$ symmetry and the specific orbital $(X^2 - Y^2)$ is shown to play a key role in stabilizing the superconducting phase as well as the antiferromagnetic phase. Furthermore, we find a one-to-one correspondence between superconductivity and enhanced uniform charge fluctuations. We also perform the analysis for the Hubbard model and find that similar one-to-one correspondence also exists in the Hubbard model [5], which is one of the simplest models for cuprates. Despite many differences between iron-based superconductors and cuprates, our study suggests that the enhanced uniform charge fluctuations play a key role in stabilizing the superconductivity in both materials. Further theoretical exploration such as examining the stability of the superconductivity in hole-doped materials such as LaMnAsO and LaMnPO is intriguing issue but is left for future study.

References

[1] For a review, see T. Miyake and M. Imada: J. Phys. Soc. Jpn. **79** (2010) 112001.

[2] T. Misawa, K. Nakamura, and M. Imada: J. Phys. Soc. Jpn. **80** (2011) 023704.

[3] T. Misawa, K. Nakamura, and M. Imada: Phys. Rev. Lett. **108** (2012) 177007.

[4] T. Misawa and M. Imada: Nat. Commun. **5** (2014) 5738.

[5] T. Misawa and M. Imada: Phys. Rev. B **90** (2014) 1115137.

Non-equilibrium phase transitions in superconductors and electron-phonon systems

Hideo AOKI
Department of Physics, University of Tokyo
Hongo, Tokyo 113-0033

Thermalization crossover in electron-phonon systems[1]

We study the relaxation of the Holstein model, a simplest possible electron-phonon system, after a sudden switch-on of the interaction with the nonequilibrium dynamical mean field theory (DMFT)[1]. We show that, on the weaker interaction side the phonon oscillations are damped more rapidly than the electron thermalization time scale, while converse is true in the stronger interaction regime. In equilibrium, we have shown that the phase diagram contains a supersolid phase accompanied by a quantum critical point.[2]

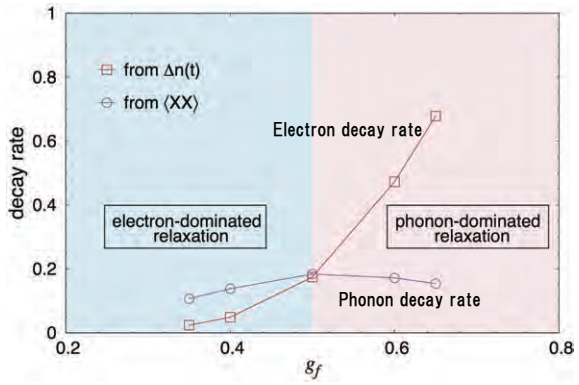

Figure 1: Thermalization crossover[1].

Nonequilibrium dynamical mean-field theory and its cluster extension[3, 4]

Nonequilibrium DMFT is one of the most powerful approaches to deal with nonequilibrium correlated many-body systems, as we have reviewed in Ref.[3]. We have also proposed the nonequilibrium dynamical cluster approximation (DCA) [4], in which the lattice model is mapped to a multi-site cluster. We have applied it to the one- and two-dimensional Hubbard models.

Topological Mott insulator in cold atoms on an optical lattice[5]

We design for fermionic cold atoms in an optical lattice a spontaneous symmetry breaking induced by the inter-atom interaction into a topological Chern insulator in a continuous space. Such a state, sometimes called the topological Mott insulator (TMI), requires, in the tight-binding model, unusually large off-site interactions. Here we overcome the difficulty by introducing a spin-dependent potential, where a sizeable inter-site interaction is achieved by a shallow optical potential. We employ the density functional theory for cold-atoms, here extended to accommodate non-collinear spin structures emerging in the topological regime, to quantitatively demonstrate the phase transition to TMI.

Light-induced collective pseudospin precession resonating with Higgs mode in a superconductor[6, 7]

We show that a strong light field can induce oscillations of the superconducting order parameter with twice the frequency $\Omega =$ of the terahertz field. This is a collective pre-

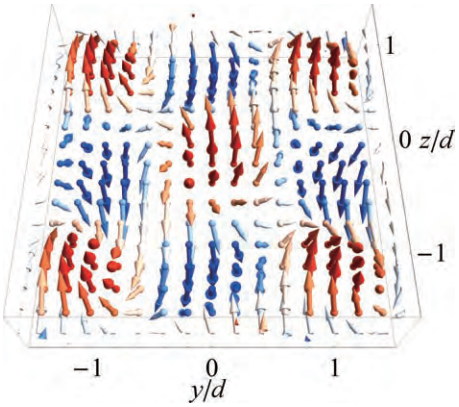

Figure 2: Spatial texture of the magnetization (arrows) for the designed topological Mott insulator[5].

cession of Anderson ' s pseudospins in ac driving fields through a nonlinear light-matter coupling, and experimentally detected in NbN. Furthermore, a resonance between the field and the Higgs amplitude mode of the superconductor is shown to occur at 2Ω = the superconducting gap. This produces a large third-harmonic generation, which is also experimentally verified. We have then examined this more accurately in the attractive Hubbard model with the nonequilibrium DMFT to endorse that the resonance for the third harmonic generation does remain.

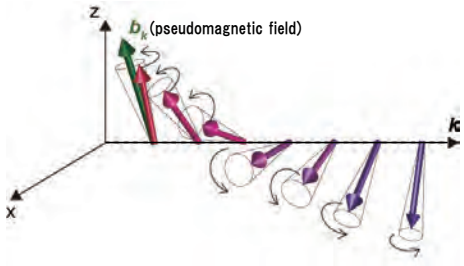

Figure 3: A schematic picture of the pseudospin precession in the Higgs mode in a superconductor.[6]

References

[1] Yuta Murakami, Philipp Werner, Naoto Tsuji and Hideo Aoki: Interaction quench in the Holstein model: Thermalization crossover from electron- to phonon-dominated relaxation, *Phys. Rev. B* **91**, 045128 (2015).

[2] Yuta Murakami, Philipp Werner, Naoto Tsuji and Hideo Aoki: Supersolid phase accompanied by a quantum critical point in the intermediate coupling regime of the Holstein model, *Phys. Rev. Lett.* **113**, 266404 (2014).

[3] Hideo Aoki, Naoto Tsuji, Martin Eckstein, Marcus Kollar, Takashi Oka and Philipp Werner: Nonequilibrium dynamical mean-field theory and its applications, *Rev. Mod. Phys.* **86**, 779 (2014).

[4] Naoto Tsuji, Peter Barmettler, Hideo Aoki and Philipp Werner: Nonequilibrium dynamical cluster theory, *Phys. Rev. B* **90**, 075117 (2014).

[5] S. Kitamura, N. Tsuji and H. Aoki: An interaction-driven topological insulator in fermionic cold atoms on an optical lattice: A design with a density functional formalism, arXiv:1411.3345.

[6] Ryusuke Matsunaga, Naoto Tsuji, Hiroyuki Fujita, Arata Sugioka, Kazumasa Makise, Yoshinori Uzawa, Hirotaka Terai, Zhen Wang, Hideo Aoki, and Ryo Shimano: Light-induced collective pseudospin precession resonating with Higgs mode in a superconductor, *Science* **345**, 1145 (2014).

[7] Naoto Tsuji and Hideo Aoki: Theory of Anderson pseudospin resonance with Higgs mode in a superconductor, arXiv:1404.2711.

Insulating state of multi-orbital electronic system with strong spin-orbit coupling

Toshihiro SATO
Computational Condensed Matter Physics Laboratory, RIKEN
Wako, Saitama 351-0198, Japan

Recently, many experimental studies have reported interesting behaviors of $5d$ transition-metal Ir oxides. These materials show a strong spin orbit coupling (SOC) with an electron correlation and the SOC splits the t_{2g} bands with the low-spin state in the crystal field into the effective local angular momentum $J_{\rm eff} = 1/2$ doublet and $J_{\rm eff} = 3/2$ quartet bands. The well-known material is Sr_2IrO_4 with totally five electrons in the t_{2g} bands and $J_{\rm eff} = 1/2$ antiferromagnetic (AF) insulator, indication of the half-filled $J_{\rm eff} = 1/2$ and full-filled $J_{\rm eff} = 3/2$ bands, has been observed[1, 2, 3, 4]. However, the ground state of multi-orbital systems with the competition between the electron correlations and the SOC has not been well understood.

We study electronic structure of the three-orbital Hubbard model with the full Hund' rule coupling and the SOC terms at five electrons filling

$$
\begin{aligned}
H &= \sum_{\langle i,j\rangle,\gamma,\sigma} t^{\gamma} c^{\gamma\dagger}_{i\sigma} c^{\gamma}_{j\sigma} - \sum_{i,\gamma,\sigma} \mu^{\gamma} n^{\gamma}_{i\sigma}, \\
&+ U \sum_{i,\gamma} n^{\gamma}_{i\uparrow} n^{\gamma}_{i\downarrow} + \frac{U'-J}{2} \sum_{i,\gamma\neq\delta,\sigma} n^{\gamma}_{i\sigma} n^{\delta}_{i\sigma} \\
&+ \frac{U'}{2} \sum_{i,\gamma\neq\delta,\sigma} n^{\gamma}_{i\sigma} n^{\delta}_{i\bar{\sigma}} - J \sum_{i,\gamma\neq\delta} c^{\gamma\dagger}_{i\uparrow} c^{\gamma}_{i\downarrow} c^{\delta\dagger}_{i\downarrow} c^{\delta\dagger}_{i\uparrow} \\
&+ J' \sum_{i,\gamma\neq\delta} c^{\gamma\dagger}_{i\uparrow} c^{\gamma\dagger}_{i\downarrow} c^{\delta}_{i\downarrow} c^{\delta}_{i\uparrow} \\
&+ \lambda \sum_{\imath,\gamma,\delta,\sigma,\sigma'} \langle\gamma|\mathbf{L}_i|\delta\rangle \cdot \langle\sigma|\mathbf{S}_i|\sigma'\rangle c^{\gamma\dagger}_{i\sigma} c^{\delta}_{i\sigma'},
\end{aligned}
$$

where t^{γ} is the nearest-neighbor hopping amplitude with orbital $\gamma = (yz, zx, xy)$ and μ^{γ} is the chemical potential. U (U') is the intra-orbital (inter-orbital) Coulomb interaction and J (J') is the Hund' s (pair-hopping) coupling,

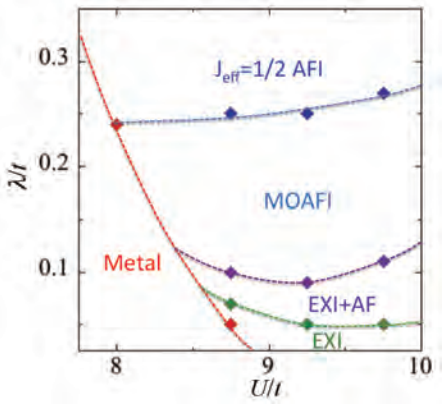

Figure 1: U-λ phase diagram at $T = 0.06t$. (MO)AFI and EXI show antiferromagnetic insulating and excitonic insulating phases, respectively.

and we set $U = U' + 2J$ and $J = J' = 0.15U$. λ is the SOC and $\mathbf{L}_i$ ($\mathbf{S}_i$) is the orbital (spin) angular momentum operator at site i. $c^{\gamma\dagger}_{i\sigma}$ ($c^{\gamma}_{i\sigma}$) is an electron creation (annihilation) operator with spin σ and orbital γ at site i and electron density operator is $n^{\gamma}_{i\sigma} = c^{\gamma\dagger}_{i\sigma} c^{\gamma}_{i\sigma}$. By using the dynamical mean field theory [5] employing a semielliptic bare density of states with the equal bandwidth ($t^{\gamma} = t$) for t_{2g} bands and the continuous-time quantum Monte Carlo solver based on the strong coupling expansion [6], we investigated the phase diagram in the parameter space of λ and U at temperature T fixed. This numerical calculation was performed by the numerical computations using facilities at Supercomputer Center in ISSP, e.g., for $\lambda = 0.1t$, $U = 8t$, and $T = 0.06t$, about 10^8 Monte Carlo sweeps and averaging over 64 samples, and the self-consistency loop of the DMFT converges about 100 hours.

Figure 1 presents the U-λ phase diagram at

the lowest temperature $T = 0.06t$. Increasing λ at $U = 8t$ fixed, we confirmed the transition from metallic to insulating state with a magnetic order. The insulator shows $J_{\text{eff}} = 1/2$ AF insulator. Moreover, we found that excitonic insulator by the electron-hole paring between $J_{\text{eff}} = 1/2$ and $J_{\text{eff}} = 3/2$ bands is realized by λ at larger U, in addition to the $J_{\text{eff}} = 1/2$ AF insulator [7].

This work was done in collaboration with Dr. T. Shirakawa and Dr. S. Yunoki.

References

[1] B. J. Kim *et al.*: Phys. Rev. Lett. **101** (2008) 076402.

[2] B. J. Kim *et al.*: Science **323** (2009) 1329.

[3] K. Ishii *et al.*: Phys. Rev. B **83** (2011) 115121.

[4] H. Watanabe *et al.*: Phys. Rev. Lett. **105** (2010) 216410.

[5] G. Kotliar *et al.*: Phys. Rev. Lett. **87** (2001) 186401.

[6] P. Werner *et al.*: Phys. Rev. Lett. **97** (2006) 076405.

[7] T. Sato *et al.*: Phys. Rev. B **91** (2015) 124122.

Electric transport near the antiferromagnetic transition in a square-lattice Hubbard model

Toshihiro SATO
Computational Condensed Matter Physics Laboratory, RIKEN
Wako, Saitama 351-0198, Japan

As for strongly correlated electronic systems, it is interesting to investigate how magnetic frustration influences the electronic transport. This is the main issue of our work and we study optical conductivity near the magnetic transition in strongly correlated electronic systems.

The model to study is the one-band Hubbard Hamiltonian on a square lattice at half filling

$$H = -t \sum_{\langle i,j\rangle,\sigma} c^{\dagger}_{i\sigma} c_{j\sigma} + U \sum_{i} n_{i\uparrow} n_{i\downarrow} - \mu \sum_{i,\sigma} n_{i\sigma},$$

where t is the nearest-neighbor hopping amplitude, U is the on-site Coulomb repulsion and μ is the chemical potential. $c^{\dagger}_{i\sigma}(c_{i\sigma})$ is the electron creation (annihilation) operator at site i with spin σ and $n_{i\sigma}$=$c^{\dagger}_{i\sigma}c_{i\sigma}$. We focused on the electric transport and computed optical conductivity, particularly near the magnetic transition based on the cluster dynamical mean field theory (CDMFT) [1] employing a four-site square cluster. The numerical solver is the continuous-time quantum Monte Carlo (CTQMC) method based on the strong coupling expansion[2]. Furthermore, in order to investigate the effect of magnetic fluctuation to electronic transport, we have proceeded the formation of optical conductivity including vertex corrections in CDMFT both magnetic and paramagnetic states based on the Ref. [3]. This is a big challenge in numerical computations and was performed by the large-scale numerical computations using facilities at Supercomputer Center in ISSP, e.g., for $U = 6.5t$ at temperature $T = 0.42t$ in the paramagnetic phase, about 10^8 Monte Carlo sweeps and averaging over 1024 samples, which take about 96 hours.

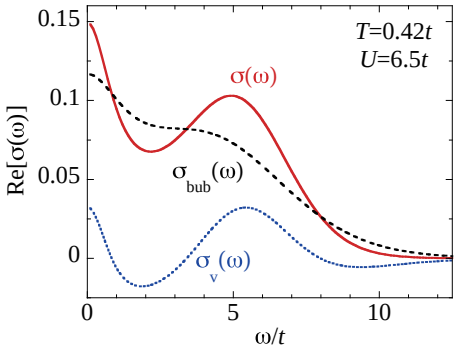

Figure 1: Contributions of vertex corrections on $\sigma(\omega)$.

We first examined T-dependence of electronic structure at $U = 6.5t$ fixed, and then confirmed that a staggered magnetization is finite below $T = 0.35t$. We have calculated the optical conductivity $\sigma(\omega)$ near $T = 0.35t$ and have examined the contribution of vertex corrections in detail. Figure 1 presents the contributions of vertex corrections; $\sigma(\omega)$ is the result with vertex corrections, $\sigma_{\rm bub}(\omega)$ is the result without vertex corrections, and the contribution of vertex corrections is $\sigma_{\rm v}(\omega) = \sigma(\omega) - \sigma_{\rm bub}(\omega)$. The data for $T = 0.42t$ are typical result on the paramagnetic states. We found that the contribution of vertex corrections is important. Vertex corrections change two peaks near $\omega \sim 0$ and $\omega \sim Ut$ into a larger weight and a narrower width. We have also confirmed that the contribution of vertex corrections is important for T-dependence of dc-conductivity $\sigma_0 = \sigma(0)$. In the future, we will investigated optical conductivity including vertex corrections below $T = 0.35t$ and will discuss the effect of magnetic fluctuation to electronic transport through detailed analysis of the contribution of vertex corrections.

This work was done in collaboration with Prof. H. Tsunetsugu.

References

[1] G. Kotliar *et al.*: Phys. Rev. Lett. **87** (2001) 186401.

[2] P. Werner *et al.*: Phys. Rev. Lett. **97** (2006) 076405.

[3] T. Sato *et al.*: Phys. Rev. B **86** (2012) 235137.

Theoretical study on the correlation between the spin fluctuation and T_c in the isovalent-doped 1111 iron-based superconductors

Hayato Arai and Yuki Fuseya
Dept. Engineering Science, University of Electro-Communications
1-5-1 Chofugaoka, Chofu, Tokyo 182-8585

The mechanism of the iron-based superconductors has been studied since $LaFeAsO_{1-x}F_x$ was found[1]. One of the possible mechanisms would be the spin-fluctuation mechanism[2]. But the low-energy spin fluctuation characterized by the relaxation rate ($1/T_1$) of NMR study seems to have no relationship to the transition temperature (T_c)[3]. Therefore it is of prime importance to understand the relationship between T_c and the spin fluctuation measured by $1/T_1$.

The isovalent doping provides the rich electron system for the iron-pnictide. It has been found that LnFeAs$O_{1-x}F_x$ with (Ln=Gd, Sm, Ce, La) has high T_c. This lanthanoid-doping enable us to control the Fe-As-Fe bond angle. Large amount of electrons can be doped by substituting O with H in LnFeAsO (Ln=Gd, Sm, Ce, La). Surprisingly, it has been shown that the superconductivity appears even up to 40% of electron doping. Particularly in LaFeAs(O,H)[4] and SmFe(As,P)(O,H)[5], the phase diagram exhibits a double-dome structure as a function of the electron doping. These experimental findings suggest that the change of electronic structure due to the Fe-As-Fe bond angle is responsible for T_c.

The conventional five-orbital model whose Fe-As-Fe bond angle is the controllable parameter are constructed based on the most localized Wannier functions. We study the electron structure, finite energy spin fluctuation, and T_c for this five-orbital model of isovalent-doped 1111 iron-based superconductors on the basis of the fluctuation exchange approximation (FLEX). We also calculate the eigenvalue of the Eliashberg equation under the $s^{\pm}$ projection ($\lambda^{\pm}$). Their self-consistent calculations are too heavy to carry out by the workstation in our laboratory, so we need to calculate by using the ISSP system.

The obtained results reveal that the higher energy spin fluctuation is responsible for T_c and lower energy spin fluctuation is for $1/T_1$. It is also found that two orbitals ($d_{xz/yz}$ and d_{xy}) of isovalent-doped 1111 iron-based superconductors is very important for superconductivity. Finally, double-dome of T_c observed in 1111 iron-based superconductor can be explained within the spin fluctuation mechanism. This work was published in Physical Review B[6].

References

[1] Y. Kamihara, T. Watanabe, M. Hirano, H. Hosono: J. Am. Chem. Soc., **130**, 3296 (2008).

[2] K. Kuroki, S. Onari, R.Arita, H.Usui, Y. Tanaka, H. Kontani, and H. Aoki , Phys. Rev. Lett. **101** (2008) 087004.

[3] H. Mukuda, F. Engetsu, K. Yamamoto, K.T. Lai, M. Yashima, Y. Kitaoka, A. Takemori, S. Miyasaka, and S. Tajima, Phys. Rev. B **89**, 064511 (2014).

[4] S. Iimura, S. Matsuishi, H. Sato, T. Hanna, Y. Muraba, S. W. Kim, J. E. Kim, M. Takata and H. Hosono, Nat. Commun. **3**, 943 (2012).

[5] S. Matsuishi, T. Maruyama, S. Iimura, and H. Hosono, Phys. Rev. B **89**, 094510 (2014).

[6] H. Arai, H. Usui, K. Suzuki, Y. Fuseya, K. Kuroki, Phys. Rev. B. **91**, 134511 (2015).

Monte Carlo Approach to Chiral Helimagnets

Shintaro HOSHINO, Misako SHINOZAKI and Yusuke KATO
Department of Basic Science, The University of Tokyo, Meguro, Tokyo 153-8902, Japan

A chirality in magnetic materials causes antisymmetric Dzyaloshinskii-Moriya (DM) interaction in addition to the symmetric Heisenberg interaction. The competition between these two effects gives rise to a helical magnetic structure which is indeed realized in $Cr_{1/3}NbS_2$ [1]. Under the external magnetic field perpendicular to the helical chain axis, an interesting spin texture called chiral soliton lattice is developed [2].

Recent theoretical studies have treated this system as a one-dimensional chain with continuum approximation, which is known as the chiral sine-Gordon model [2]. The temperature dependence of the spin moment has been discussed phenomenologically in these works, and is in good agreement with experiments. For more quantitative description of the magnetic phase transition at fintie temperature, however, it is necessary to go beyond the one-dimensional system. To deal with this issue, we take classical chiral helimagnet on a three-dimensional simple cubic lattice, and numerically investigate the finite-temperature properties. The Hamiltonian reads

$$\mathscr{H} = -\sum_{\langle ij \rangle} J_{ij} \boldsymbol{S}_i \cdot \boldsymbol{S}_j - \sum_{\langle ij \rangle} \boldsymbol{D}_{ij} \cdot (\boldsymbol{S}_i \times \boldsymbol{S}_j)$$

where the summation is taken over the nearest neighbor sites. We consider the ferromagnetic interaction $J_{ij} > 0$, and take $J_{ij} = J^{\parallel}$ ($J^{\perp}$) for the z-axis (x, y-axis) bond. On the other hand, the DM interaction is given by $\boldsymbol{D}_{ij} = (0, 0, D)$ for the z-axis bond, and is zero for x- and y-axis bonds. This model is simulated by the heat-bath method [3] using the facilities of the system B. In order to improve the accuracy, we additionally apply the exchange Monte Carlo method [4].

Figure 1 shows the transition temperature T_c obtained by the Monte Carlo method (circle symbols). Here we take $D/J^{\parallel} = 0.16$ which is relevant to $Cr_{1/3}NbS_2$. For comparison, the mean-field result is shown by red line, which have the higher transition temperature. We have also analyzed the system by simulating the xy-plane using the Monte Carlo method and treating the interactions along z-axis by the mean-field approximation. As shown by square symbols in Fig. 1, much better results are obtained compared to the fully mean-field description.

In addition to T_c, we have also estimated the value of the critical field where the chiral soliton lattice turns into the forced ferromagnetic state at zero temperature. By comparing our numerical results with the experimental data, we have derived the energy scales of the interaction parameters in $Cr_{1/3}NbS_2$.

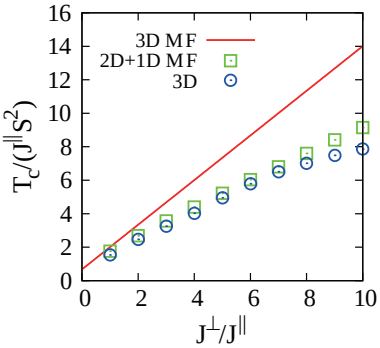

Figure 1: $J^{\perp}$-dependence of the transition temperatures in the chiral helimagnet.

References

[1] T. Moriya and T. Miyadai, Solid State Commun. **42**, 209 (1982).

[2] J. Kishine, K. Inoue, and Y. Yoshida, Prog. Theor. Phys. Suppl. **159**, 82 (2005).

[3] Y. Miyatake *et al.*, J. Phys. C: Solid State Phys. **19**, 2539, (1986).

[4] K. Hukushima and K. Nemoto, J. Phys. Soc. Jpn. **65**, 1604 (1996).

Quantum Monte Carlo simulation and electronic state calculations in correlated electron systems

Takashi YANAGISAWA
Electronics and Photonics Research Institute
National Institute of Advanced Industrial Science and Technology (AIST)
AIST Central 2, 1-1-1 Umezono, Tsukuba 305-8568

Superconductivity and Strong Correlation

The mechanisms of superconductivity in cuprate high-temperature superconductors have been extensively studied by using two-dimensional models of electronic interactions. To clarify the electronic state of CuO_2 plane in cuprates is important to resolve the mechanism of superconductivity. It is well known that the parent materials are a Mott insulator and the hole doping leads to superconductivity. In this report we present the results on the d-p model. To use computers more e ciently, we performed parallel computing with 64 or 128 cores.

The three-band model that explicitly includes Oxygen p orbitals contains the parameters $U_{\rm d}$, $U_{\rm p}$, $t_{\rm dp}$, $t_{\rm pp}$, $_d$ and $_{\rm p}$. $U_{\rm d}$ is the on-site Coulomb repulsion for d electrons and $U_{\rm p}$ is that for p electrons. $t_{\rm dp}$ is the transfer integral between adjacent Cu and O orbitals and $t_{\rm pp}$ is that between nearest p orbitals. The energy unit is given by $t_{\rm dp}$.

The wave function is the Gutzwiller-type wave function given by the form $_G = P_G\ _0$, where P_G is the Gutzwiller projection operator given by $P_G = \prod_i [1 \quad (1 \quad g) n_{di\uparrow} n_{di\downarrow}]$ with the variational parameter in the range from 0 to unity. P_G controls the on-site electron correlation on the copper site. $_0$ is a one-particle wave function such as the Fermi sea or the Hartree-Fock state with spin density wave. $_0$ contains the variational parameters $\tilde{t}_{dp}$, $\tilde{t}_{pp}$, $\tilde{}_d$ and $\tilde{}_p$: $_0 = \ _0(\tilde{t}_{dp}, \tilde{t}_{pp}, \tilde{}_d, \tilde{}_p)$. In the non-interacting case, $\tilde{t}_{dp}$ and $\tilde{t}_{pp}$ coincide with t_{dp} and t_{pp}, respectively.

The subject whether there is a superconducting instability induced by the on-site Coulomb repulsion is still controversial although there have been many works on the Hubbard model. In my opinion, high-temperature superconductivity can be expected in the strongly correlated region in the Hubbard model or the d-p model. In the two-dimensional Hubbard model, the ground state goes into a strongly correlated region when U/t is beyond 7, i.e. $U_{\rm c}/t \quad 7$. The superconducting condensation energy $E_{\rm cond}$ increases rapidly near $U/t \quad 7$ and has a maxmum at $U/t \quad 12$ as shown in Fig.1. Here, $E_{\rm cond}$ is de ned as $E_{\rm cond} = E_{\rm normal} \quad E_{\rm g}(\ )$ where $E_{\rm normal}$ is the energy of the normal state and $E_{\rm g}(\ )$ is the minumum of the energy when we introduced the superconducting gap function .

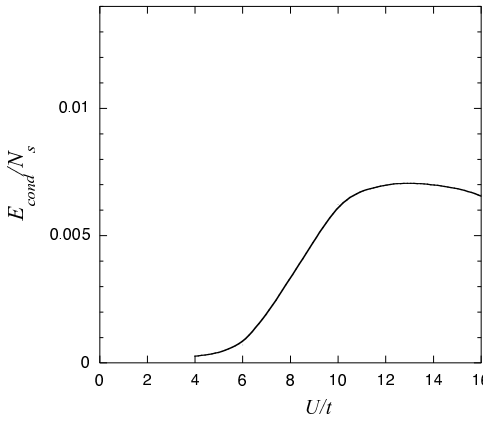

Figure 1: Superconducting condensation energy of the 2D Hubbard model as a function U. Parameters are $t'/t = \ 0.2$ and the electron density is $n_{\rm e} = 0.84$. The system size is 10 10. We assumed the d-wave pairing for the gap function.

Let us examine the two-dimensional d-p model where the subject is whether the strongly correlated region exists in the d-p model. We expect that the superconducting correlation function is enhanced in the strongly correlated region.

The Fig.2 exhibits the ground state energy per site E/N $_d$ in the half- lled case as a function of $_{dp}$ $_p$ $_d$ for the d-p model. Here we adopt the wave function given by

$$= \exp(\lambda K) \ _G, \qquad (1)$$

where K is the kinetic part of the total Hamiltonian H_{dp} and λ is a variational parameter. We can nd that the curvature of the energy, as a function of $_{\rm dp}$, is changed near $_{\rm dp}$ 2. The energy is well tted by $1/\ _{\rm dp}$ shown by the dashed curve when $_{\rm dp}$ is large. This is because the most energy gain comes from the exchange interaction between nearest neighbor d and p electrons. This exchange interaction, denoted by $J_{\rm K}$, is given by $J_K = t_{\rm dp}^2(1/\ _{\rm dp} + 1/(U_{\rm d}\ \ _{\rm dp}))$. In the insulating state the energy gain is proportional to $J_{\rm K}$,

$$E = \frac{E}{N}\ \ _d \propto \ \ J_{\rm K}. \qquad (2)$$

The critical value of $_{\rm dp}$ is $(\ \ _{\rm dp})_c \simeq 3t_{\rm dp}$.

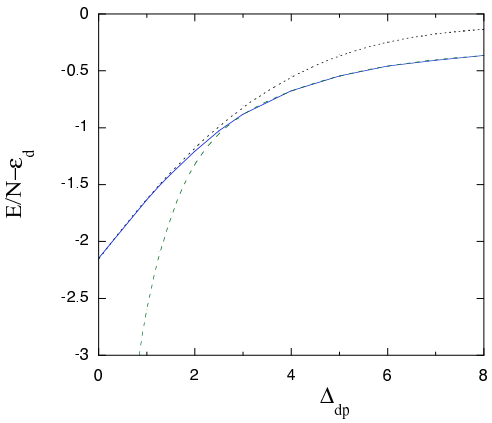

Figure 2: Ground-state energy of the 2D d-p model at half- llig as a function of $_{\rm dp}$ for $t_{\rm pp} = 0.0$ and $U_{\rm d} = 8$ in units of $t_{\rm dp}$. The calculations were performed on 6 6 lattice. The dotted curve is for the Gutzwiller function with $\lambda = 0$.

As shown in Fig.2, the region for $_{\rm dp}$ being largeer than the critial value 3 $4t_{\rm dp}$ may be regarded as the strongly correlated region. We examine our question: whether the superconducting correlation is enhanced in the strongly correlated region in the d-p model as for the 2D Hubbard model. We found that the the d-wave pairing state is indeed stabilized in the region with large $_{\rm dp}$. The condensation energy $E_{\rm cond}$ shows a rapid increase as $_{\rm dp}$ is increased beyond the critical value $_{{\rm dp},c}$. The behaviour of $E_{\rm cond}$ is shown in Fig.3 as a function of the level di erence $_{\rm dp}$. This indicates a possibility of high-temperature supercoductivity in the strongly correlated region of the d-p model.

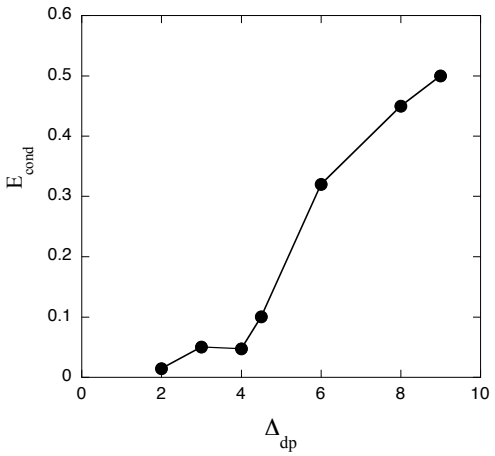

Figure 3: Superconducting condensation energy of the 2D d-p model as a function of $_{\rm dp}$ for $t_{\rm pp} = 0.4$ and $U_{\rm d} = 10$ in units of $t_{\rm dp}$. The calculations were performed on 6 6 lattice. The dotted curve is for the Gutzwiller function with $\lambda = 0$.

References

[1] T. Yanagisawa, Phys. Rev. B75, 224503 (2007) (arXiv: 0707.1929).

[2] T. Yanagisawa, New J. Phys. 15, 033012 (2013).

[3] T. Yanagisawa and M. Miyazaki, EPL 107, 27004 (2014).

Multi-variable variational Monte Carlo study of the Holstein-Hubbard model

Takahiro OHGOE
Department of Applied Physics, University of Tokyo
7-3-1, Hongo, Bunkyo-ku, Tokyo, 113-0033

Electron-phonon interaction plays important roles in various phenomena of conventional superconductor, charge density wave, and resistivity. Although its roles are well understood in those phenomena. They have not been fully understood in strongly-correlated systems such as high-T_c cuprates. Even for the Holstein-Hubbard model, which is one of the simplest models of electronphonon coupled systems, it is difficult to study its property in two or three dimensions because of limitations on methodologies. However, we have recently developed a multi-variable variational Monte Carlo method for electron-phonon coupled system [1]. In this study, we applied it to the Holstein-Hubbard model on a square lattice to reveal its zero-temperature phase diagrams. We first studied the half-filling case. In this case, we found not only spin-density wave (SDW) phase and charge-density wave (CDW) phase but also an intermediate metalic phase between them. Such an intermediate phase was also observed in the one-dimensional case [2]. To clarify whether the intermediate region includes a superconducting phase or not, we measured the superconducting correlation function, but we did not found evidence of superconductivity. In addition to the halffilling case, we next studied the system away from the half-filling. In this case, we observed the appearance of superconductivity. Moreover, we revealed the optimal filling where the superconducting order becomes largest. As a result, we could capture the overall behavior of the phase diagram. In this study, we needed to perform simulations at various different parameter sets and up to large system sizes (linear dimension $L = 16$ or 18). Therefore, we performed intensive independent simulations for different parameters. In each simulation, we utilized a MPI parallelization (# of process ~ 64) to increase the number of samples. Most of these simulations were performed on System B.

References

[1] T. Ohgoe and M. Imada, Phys. Rev. B **89**, 195139 (2014).

[2] Fehske et al., Eur. Phys. Lett. **84**, 57001 (2008).

Study of nobel quantum states in correlated electron systems with multi-degrees of freedom

Sumio ISHIHARA
Department of Physics, Tohoku University
Sendai 980-8578

Multi-degrees of freedom of electron and lattice play essential roles in magnetic, dielectric, transport and optical properties in correlated electron systems, such as transition-metal oxides, and low dimensional organic salts. In the projects (H26-Ba-0022, H26Bb-0004), we have studied numerically the novel quantum phase and non-equilibrium states in correlated systems with multi degree of freedom. The following are the list of the obtained results.

1) Transient dynamics of hole carriers injected into a Mott insulator with antiferromagnetic long-range order are studied. The theoretical framework for the transient carrier dynamics is presented based on the two-dimensional t-J model. The time dependencies of the optical conductivity spectra, as well as the one-particle excitation spectra, are calculated based on the Keldysh Green's function formalism at zero temperature combined with the self-consistent Born approximation. Time evolutions of the Green's functions are solved numerically. In the early stage after dynamical hole doping, the Drude component appears, and then incoherent components originating from hole-magnon scattering start to grow. Fast oscillatory behavior owing to coherent magnon and slow relaxation dynamics are confirmed in the spectra. The time profiles are interpreted as doped bare holes being dressed by magnon clouds and relaxed into spin polaron quasiparticle states. The characteristic relaxation times for Drude and incoherent peaks strongly depend on the momentum of the dynamically doped hole and the exchange constant [1].

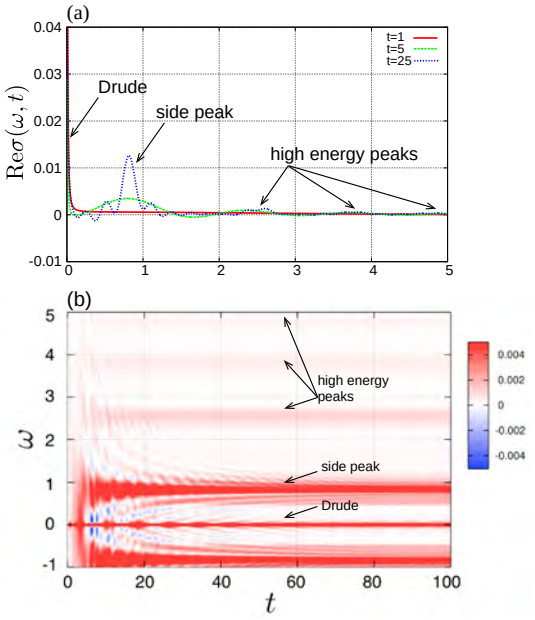

Figure 1: Transient optical conductivity spectra. (a) The spectra for several time after dynamicsl doping. (b) A contour map of the spectra as a function of frequency and time [1].

2) Photo-excited charge dynamics of interacting charge-frustrated systems are studied using a spinless fermion model on an anisotropic triangular lattice. Real-time evolution of the system after irradiating a pump-photon pulse is analyzed by the exact diagonalization method based on the Lanczos algorithm. We focus on photo-excited states in the two canonical charge-ordered (CO) ground states, i.e., horizontal stripe-type and verti-

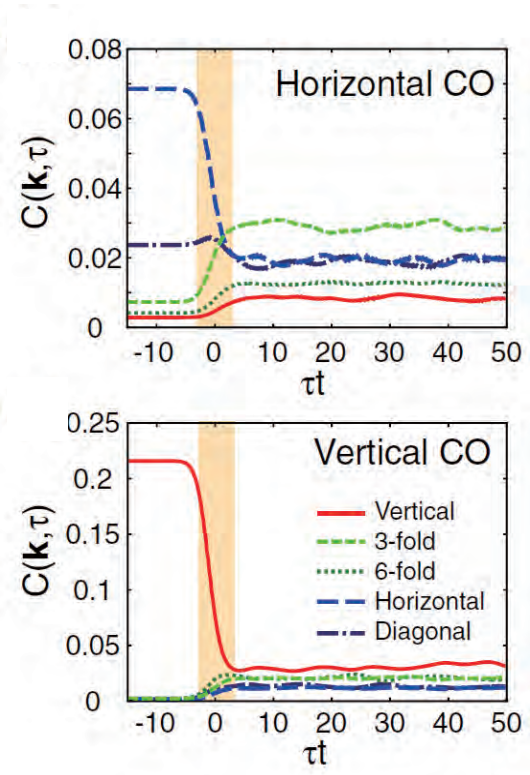

Figure 2: Time-dependences of the charge correlation functions in the horizontal-stripe and vertical-stripe CO phases [2].

cal stripe-type COs, which compete with each other owing to the charge frustration. We find that the photo-induced excited states from the two types of COs are distinct. From the horizontal stripe-type CO, a transition to another CO state called the three-fold CO phase occurs. In sharp contrast, the vertical stripe-type CO phase is only weakened by photo-irradiation. Our observations are attributable to the charge frustration effects occurring in the photo-excited states [2].

3) Short-range resonating valence-bond states in an orbitally degenerate magnet on a honeycomb lattice are studied. A quantum-dimer model is derived from the Hamiltonian which represents the superexchange interaction and the dynamical Jahn-Teller (JT) effect. We introduce two local units termed "spin-orbital singlet dimer," where two spins in a nearest-neighbor bond form a singlet state associated with an orbital polarization along the bond, and "local JT singlet," where an orbital polarization is quenched due to the dynamical JT effect. A derived quantum-dimer model consists of the hopping of the spin-orbital singlet dimers and the JT singlets, and the chemical potential of the JT singlets. We analyze the model by the mean-field approximation, and find that a characteristic phase, termed "JT liquid phase," where both the spin-orbital singlet dimers and the JT singlets move quantum mechanically, is realized [3].

The present researches has been collaborated with E. Iyoda (University of Tokyo), J. Nasu (Tokyo Institute of Technology), M. Naka (Tohoku University), H. Hashimoto (Tohoku University), H. Matsueda (Sendai National College of Technology) and H. Seo (RIKEN, CEMS). Some parts of the computation in the present works has been done using the facilities of the Supercomputer Center, the Institute for Solid State Physics, the University of Tokyo.

References

[1] E. Iyoda and S. Ishihara, Phys. Rev. B **89**, 125126 (2014).

[2] H. Hashimoto, H. Matsueda, H. Seo and S. Ishihara, J. Phys. Soc. Jpn. **83**, 123703 (2014).

[3] J. Nasu and S. Ishihara, Phys. Rev. B **91**, 045117 (2015).

Numerical study of flux quench in one-dimensional quantum systems

Yuya NAKAGAWA[1], Grégoire MISGUICH[2], Masaki OSHIKAWA[1]
[1] *Institute for Solid State Physics, University of Tokyo*
Kashiwa-no-ha, Kashiwa, Chiba 277-8581
[2] *Institut de Physique Théorique, CEA, IPhT,*
CNRS, URA 2306, F-91191 Gif-sur-Yvette, France

We study a *flux quench* problem in the spin-1/2 XXZ chain. The flux quench is a quantum quench where the flux ϕ piercing the XXZ chain is turned off at $t = 0$ suddenly. If we formulate the XXZ chain as a spinless fermion model, the flux ϕ corresponds to a vector potential on each bond and this flux quench can be viewed as imposing a pulse (delta function) of electric field. Therefore some particle (or spin) current is generated in the system at $t = 0$. Recently this quench was studied to illustrate the breakdown of the generalized Gibbs ensemble in integrable systems [1].

Here, we focus on the time-evolution of the spin current after the quench and calculate it numerically by the infinite time-evolving block decimation (iTEBD) method [2]. We used the bond dimension $\chi = 1000$ typically, and did numerical simulations for various parameters of the system (the anisotropy of the XXZ chain and the initial flux). We implemented $U(1)$ symmetry (the conservation of magnetization) to the iTEBD algorithm so as to reduce the computational cost of singular value decomposition.

We find that the dynamics of the spin current depends strongly on the anisotropy parameter Δ of the XXZ chain and the amount of flux initially inserted. The long-time limit ($t \to \infty$) of the current matches with predictions of linear response theory as the initial flux decreases, but the deviation from linear response theory is largely affected by the sign of interactions. Furthermore, in some parameter region the current oscillates in time (Fig. 1) and the frequency of the oscillation is proportional to $|\Delta|$. Remarkably, the dynamics of momentum distribution of the spinless fermions reveals that this oscillation of the current is governed by excitations deep inside the shifted Fermi sea (Fig. 2). This mechanism of oscillations cannot be captured by the effective Luttinger model corresponding to the microscopic XXZ chain, which is in contrast with the previous studies on different types of quench in the same model [3].

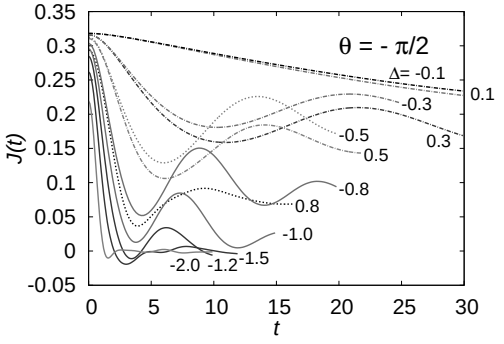

Figure 1: Dynamics of the spin current after the quench. θ is initial flux per site. Anisotropy Δ is defined as $H_{\mathrm{XXZ}} = -\sum_i \left(S_i^x S_{i+1}^x + S_i^y S_{i+1}^y + \Delta S_i^z S_{i+1}^z\right)$.

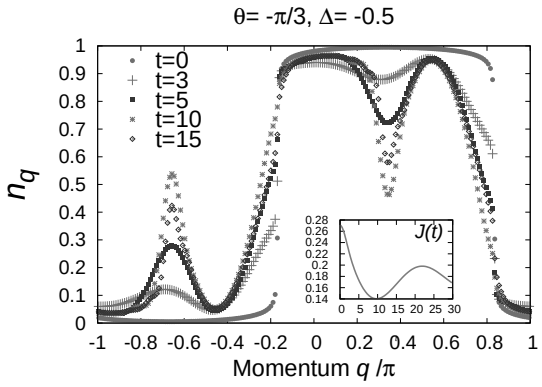

Figure 2: Momentum distribution of the spinless fermions. The dip (peak) structure deep inside the shifted Fermi sea is observed (the inset shows the time-evolution of the current).

References

[1] M. Mierzejewski, P. Prelovsek, and T. Prosen: Phys. Rev. Lett. **113** (2014) 020602.

[2] G. Vidal: Phys. Rev. Lett. **98** (2007) 070201.

[3] C. Karrasch *et al*: Phys. Rev. Lett. **109** (2012)126406., F. Pollmann, M. Haque, and B. Dóra: Phys. Rev. B **87** (2013) 041109(R).

Investigation of unconventional superconductivities by extension of the dynamical mean-field theory

Junya OTSUKI
Department of Physics, Tohoku University, Sendai 980-8578

For theoretical descriptions of superconductivities in strongly correlated systems, we need a coherent treatment of local correlations and spatial fluctuations. For this purpose, we establish a practical scheme using the dual fermion approach, which provides a way to perform a diagrammatic expansion around the dynamical mean-field theory (DMFT) [1]. The computation process consists of two auxiliary problem as summarized in Fig. 1.

We first solve an effective single-impurity problem as in the DMFT. A difference to the DMFT is that we compute the vertex part $\gamma_{\omega\omega',\nu}$ as well as the Green's function g_ω. We used the continuous-time quantum Monte Carlo (QMC) method [2], and performed parallel computations using MPI.

The quantities g_ω and $\gamma_{\omega\omega',\nu}$ define a dual-lattice problem. We evaluate the dual self-energy $\tilde{\Sigma}_{\omega\boldsymbol{k}}$ taking account of diagrams as in the fluctuation exchange approximation (FLEX). Thus, influence of long-range fluctuations are incorporated in addition to the local correlations in DMFT. We invented a way to carry out stable computations even near an antiferromagnetic quantum critical point, making possible to obtain solutions near a Mott insulator [3]. The calculation of $\tilde{\Sigma}_{\omega\boldsymbol{k}}$ was parallelized as well.

After $\tilde{\Sigma}_{\omega\boldsymbol{k}}$ is computed, we update the bath function Δ_ω and solve again the single-impurity problem. These calculations are repeated until convergence is reached. The Green's function in the original lattice, $G_{\omega\boldsymbol{k}}$, are finally obtained from $\tilde{\Sigma}_{\omega\boldsymbol{k}}$.

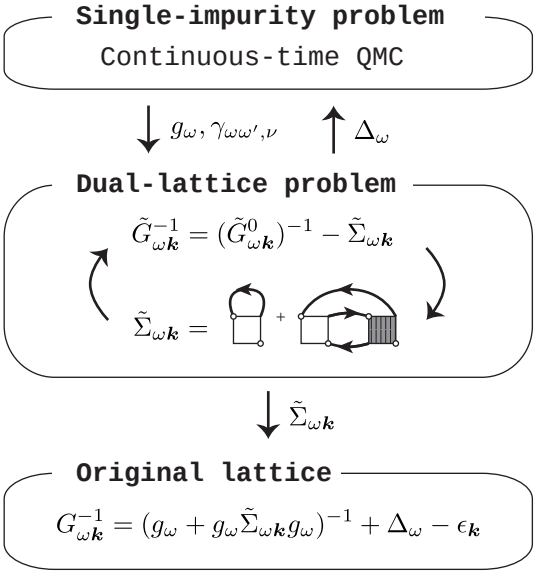

Figure 1: Computation scheme.

Applying the above scheme, we have investigated superconductivities in the two-dimensional Hubbard model. We observed d-wave superconductivity (d-SC) and phase separation (PS) near the Mott insulator [3]. It turned out that a pure d-SC emerges only in a limited doping regime because of the PS.

References

[1] A. N. Rubtsov *et al.*, Phys. Rev. B **79**, 045133 (2009).

[2] E. Gull *et al.*, Rev. Mod. Phys. **83**, 349 (2011).

[3] J. Otsuki, H. Hafermann, A. I. Lichtenstein, Phys. Rev. B **90**, 235132 (2014).

Numerical simulation of ^{4}He adsorbed on substrates

Yuichi MOTOYAMA
Institute for Solid State Physics, University of Tokyo
Kashiwa-no-ha, Kashiwa, Chiba 277-8581

^{4}He adsorbed on a substrate such as graphite has been studied experimentally and numerically as an ideal two dimensional interacting bosonic system. Although the numerical simulations of the first layer of ^{4}He on graphite almost agree with the experiments, for the second layer the latest first-principle numerical result [1] did not agree with the latest experimental result [2] even in quality. The authors of the former calculated the superfluid density and the structure factor of the number density, and concluded there are three phases; gas-liquid coexisting phase (GL), superfluid liquid phase (SF), and incommensurate solid phase (IC). The latter experiment gave anomalous behavior of the specific heat and the authors concluded that there are more phases; GL, SF, SF and commensurate solid (C) coexisting phase, C, C-IC coexisting, and IC. The specific heat is one of the important observables that can be obtained from experiments. The past simulations, however, did not show these data since it is difficult for numerical simulation to calculate energy and specific heat accurately.

Aiming to verify the past numerical simulation and fill the gap between experiments and simulations, I am developing a path-integral Monte Carlo simulation for interacting boson particles in continuous space introduced by ref [3]. In this algorithm, which was used in the past numerical paper [1], it takes time proportional to the number of particles to perform one Monte Carlo update, and so this enables us to simulate large size system. I performed simulation of two dimensional ^{4}He system for several temperature and fixed number density $\rho = 0.0432\text{Å}^{-2}$ on ISSP supercomputer system-B and examined the scaling of update time [4]. Figure 1 shows that the linear scaling of elapsed time is achieved.

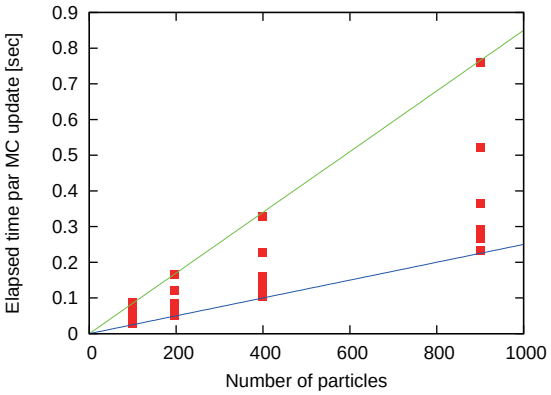

Figure 1: Elapsed time for one Monte Carlo update of two dimensional ^{4}He simulation for several temerature ($0.5\text{K} \leq T \leq 1\text{K}$). Computational cost is $\mathrm{O}(N)$ with particle number N. Two solid lines are for eye-guide.

References

[1] P. Corboz, M. Boninsegni, L. Pollet, and M. Troyer, Phys. Rev. B **78**, 245414 (2008).

[2] S. Nakamura, K. Matsui, and H. Fukuyama, arXiv:1406.4388.

[3] M. Boninsegni, N. V. Prokof'ev, and B. V. Svistunov, Phys. Rev. E **74**, 036701 (2006).

[4] I use ALPS/parapack library [5] for embarrassingly parallelization and scheduling.

[5] B. Bauer et al. (ALPS collaboration), J. Stat. Mech. P05001 (2011).

Theoretical study for exciton condensation induced by interband interaction

Hiroshi WATANABE
RIKEN CEMS
2-1, Hirosawa, Wako-shi, Saitama 351-0198

In multiband electron systems, interband interaction induces various interesting phenomena. One of the notable examples is exciton condensation which has been proposed in 1960s. The exciton is a bound electron-hole pair mediated by interband Coulomb interaction and is expected to condense in low carrier density system like semimetal or semiconductor. Although there are several candidates of exciton condensation in real materials, none of them have been confirmed so far. Since most of the previous theoretical studies are based on simplified ideal models, they are not enough to discuss the exciton condensation in real materials. Furthermore, the Coulomb interaction is treated within the mean-field approximation and the many-body effect is not appropriately included.

To discuss the possibility of exciton condensation in real materials, we have constructed the realistic two-dimensional Hubbard model and studied the ground state property of the model [1, 2]. The variational Monte Carlo (VMC) method is used for the calculation of physical quantities. Our VMC code includes more than one hundred variational parameters and the many-body effect is much more properly included compared with mean-field approximation. The system size for calculation is from 8×8 to 28×28 and the size dependence is systematically studied.

We have found three phases in the ground state phase diagram of intra- (U/t) and interband (U'/t) Coulomb interactions in the unit of nearest-neighbor hopping integral t [1] (Fig. 1): paramagnetic metal (PM), excitonic insulator (EI) originated from exciton condensation, and band insulator (BI). The transition from PM to EI is induced by an infinitesimal interband Coulomb interaction, i.e., $U'_c = 0$ (Fig. 1), when the electron and hole Fermi surfaces are perfectly nested in a square lattice. As U' increases, the character of exciton changes from weak-coupling BCS-type to strong-coupling BEC-type pairing within EI, which is known as BCS-BEC crossover. As U' increases further, EI finally collapses and BI appears. On the other hand, EI is absent and direct transition from PM to BI is observed in

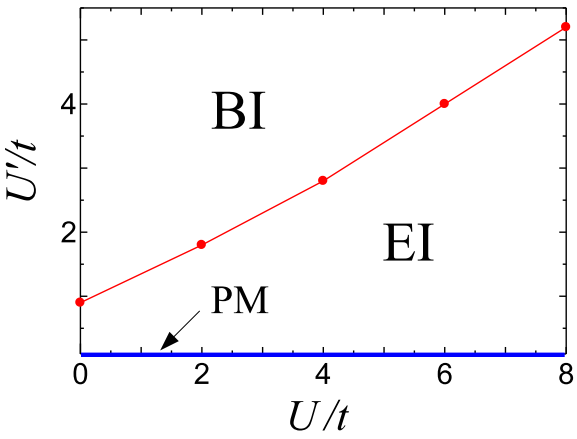

Figure 1: Ground state phase diagram for the Hubbard model in a square lattice with perfectly nested electron and hole Fermi surfaces [1].

a triangular lattice [2]. It suggests that the stability of EI greatly depends on the nesting of the Fermi surface. In real materials, the nesting of the Fermi surface is not perfect and the realization of EI would be limited to a special case. Our result will contribute to the further understanding and realization of exciton condensation in real materials.

References

[1] H. Watanabe, K. Seki, and S. Yunoki: J. Phys.: Conf. Ser. **592** (2015) 012097.

[2] H. Watanabe, K. Seki, and S. Yunoki: submitted to Phys. Rev. B.